Journal of Instrumentation

SISSA

OPEN ACCESS

Mechanical stability of the CMS strip tracker measured with a laser alignment system

To cite this article: A.M. Sirunyan *et al* 2017 *JINST* **12** P04023

View the article online for updates and enhancements.

IOP ebooks™

Bringing together innovative digital publishing with leading authors from the global scientific community.

Start exploring the collection–download the first chapter of every title for free.

This content was downloaded from IP address 151.97.200.161 on 19/05/2020 at 10:59

Jinst

Published by IOP Publishing for Sissa Medialab

Received: *January 8, 2017*
Accepted: *April 8, 2017*
Published: *April 21, 2017*

Mechanical stability of the CMS strip tracker measured with a laser alignment system

The CMS collaboration

E-mail: cms-publication-committee-chair@cern.ch

Abstract: The CMS tracker consists of 206 m^2 of silicon strip sensors assembled on carbon fibre composite structures and is designed for operation in the temperature range from −25 to +25°C. The mechanical stability of tracker components during physics operation was monitored with a few μm resolution using a dedicated laser alignment system as well as particle tracks from cosmic rays and hadron-hadron collisions. During the LHC operational period of 2011–2013 at stable temperatures, the components of the tracker were observed to experience relative movements of less than 30 μm. In addition, temperature variations were found to cause displacements of tracker structures of about 2 μm/°C, which largely revert to their initial positions when the temperature is restored to its original value.

Keywords: Detector alignment and calibration methods (lasers, sources, particle-beams); Large detector systems for particle and astroparticle physics; Particle tracking detectors; Particle tracking detectors (Solid-state detectors)

ArXiv ePrint: 1701.02022

© CERN 2017 for the benefit of the CMS collaboration, published under the terms of the Creative Commons Attribution 3.0 License by IOP Publishing Ltd and Sissa Medialab srl. Any further distribution of this work must maintain attribution to the author(s) and the published article's title, journal citation and DOI.

doi:10.1088/1748-0221/12/04/P04023

2017 JINST 12 P04023

Contents

1 Introduction **1**

2 Mechanical design of the CMS tracker **2**

3 The laser alignment system **6**

4 Tracker alignment **9**
- 4.1 Alignment with the laser system 9
- 4.2 Alignment with particle tracks 12

5 Tracker mechanical stability **12**
- 5.1 Long-term stability 13
- 5.2 Stability during temperature variations 15

6 Summary **18**

The CMS collaboration **21**

1 Introduction

The silicon strip tracker of the CMS experiment at the CERN LHC is designed to provide precise and efficient measurements of charged particle trajectories in a solenoidal magnetic field of 3.8 T with a transverse momentum accuracy of 1–10% in the range of 1–1000 GeV/c in the central region [1]. It consists of five main subdetectors: the tracker inner barrel with inner disks (TIB and TID), the tracker outer barrel (TOB), and the tracker endcaps on positive and negative sides (TECP and TECM) [2, 3]. The silicon strip sensors have pitches varying from 80 μm at the innermost radial position of 20 cm, to 205 μm at the outermost radius of 116 cm, delivering a single-hit resolution between 10 and 50 μm [1]. As a general criterion, the position of the silicon modules has to be known to much better accuracy than this intrinsic resolution.

Silicon sensors exposed to a large radiation fluence require cooling, and the CMS tracker is designed to operate in a wide temperature range from −25 to +25°C. The mechanical stability of the tracker components is ensured by the choice of materials and by an engineering design that tolerates the expected thermal expansion and detector displacements. These displacements have to be measured and accounted for in the form of alignment constants used in the track reconstruction.

The absolute alignment of individual silicon modules is performed with cosmic ray muons and tracks from hadron-hadron collisions collected during periods of commissioning or collision data taking [4–6]. A significant advance in the track-based alignment came with the introduction of a global χ^2 algorithm that combines reconstruction of the track and alignment parameters [7]. This algorithm, implemented in the MILLEPEDE package [8], was successfully used in various experiments at the LHC, HERA, and Tevatron. The actual accuracy of the track-based alignment depends on the number of objects requiring alignment and the size of the track sample.

The movement of the tracker components over much shorter time scales is monitored in the CMS experiment with an optical laser alignment system (LAS) [9]. Lasers were already used in the

2017 JINST 12 P04023

alignment of several silicon-based tracking detectors, for example, in the ALEPH [10], ZEUS [11], and AMS02 [12] experiments. Moreover, the CMS experiment also uses lasers for linking the tracker and muon subdetectors together in a common reference frame [13]. There is an alternative method of optical alignment based on the RasNiK system that was implemented, for example, in the CDF [14] and ATLAS [15] experiments. The RasNik system uses a conventional light source with coded mask, a lens, and a dedicated optical sensor. Both methods have similar performance, but lasers have some advantages for operation in the CMS tracker. First, the infrared laser light penetrates the silicon sensors, hence simplifying the alignment system. Second, the laser light produces a signal similar to ionizing particles that permits the use of the same radiation-hard silicon detectors employed for tracking, instead of dedicated sensors. Yet another method, implemented in the ATLAS experiment, is based on the laser frequency scanning interferometry [16].

The LAS of the CMS tracker is one of the largest laser-based alignment systems ever built in high-energy physics. Forty infrared laser beams illuminate a subset of 449 silicon modules, and monitor relative displacements of the TIB, TOB, and TEC subdetectors over a time interval of a few minutes with a stability of a few μm [9]. Alignment with particle tracks and laser beams are complementary techniques and together they ensure the high quality of track reconstruction. While the track-based alignment is used to reconstruct the alignment constants of individual modules, the LAS identifies short-term displacements of large structures in order to exclude such periods from the offline analysis of the experimental data.

In this paper we describe the mechanical structure of the tracker and the LAS in detail. We review the alignment procedure of using laser beams and particle tracks. The measurements of the mechanical stability of the tracker components during the LHC data taking period in 2011–2013, as well as during the LHC long shutdown period spanning 2013–2014, are presented and discussed.

2 Mechanical design of the CMS tracker

The silicon strip tracker of the CMS detector is composed of 15 148 silicon strip detector modules with a total area of about 206 m^2 and is described in refs. [2, 3]. Below we discuss in more detail the components of the tracker that are relevant to the mechanical stability of the detector. The mechanical concept of the tracker is sketched in figure 1. The CMS coordinate system has its origin at the centre of the detector with the z-coordinate along the LHC beam pipe, in the direction of the counterclockwise proton beam, and the horizontal x- and the vertical y-coordinates perpendicular to the beam (in the cylindrical system r is the radial distance and φ is the azimuth). The inner radii from 4.4 up to 15 cm are occupied by the silicon pixel detector, which is operated independently of the strip tracker. The silicon strip modules are mounted around the beam pipe at radii from 20 cm to 116 cm inside a cylinder of 2.4 m in diameter and 5.6 m in length. The TIB extends in z to $\pm$70 cm and in radius to 55 cm. It is composed of two half-length barrels with four detector layers, supplemented by three TID disks at each end. The TID disks are equipped with wedge-shaped silicon detectors with radial strips. The TOB surrounds the TIB+TID. It has an outer radius of 116 cm, ranges in $|z|$ up to 118 cm, and consists of six barrel layers. In the barrel part of the tracker, the detector strips are oriented along the z-direction, except for the double-sided stereo modules in the first two layers of the TIB and TOB, where they are rotated at an angle of 100 mrad, providing reconstruction of the z-coordinate. The TECP and TECM cover the region $124 < |z| < 282$ cm

2017 JINST 12 P04023

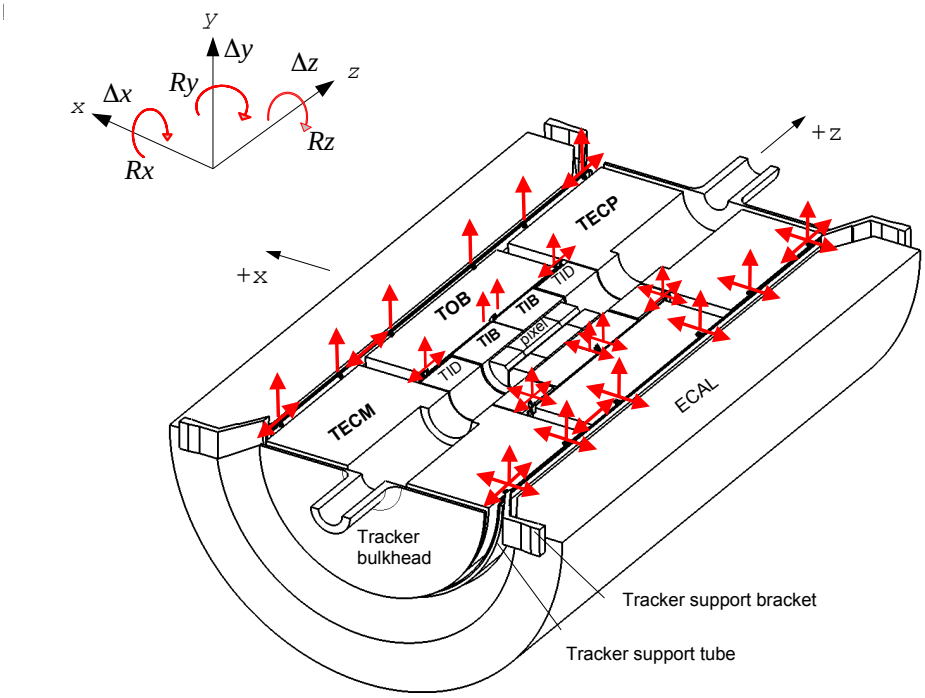

Figure 1. Mechanical layout and mounting of the tracker subdetectors (bottom half is shown). The TIB+TID are mounted inside the TOB, while the TOB, TECP, and the TECM are mounted inside the TST. The red arrows indicate the connection points and their kinematic constraints.

and $22.5 < r < 113.5$ cm. Each TEC is composed of nine disks, carrying up to seven rings of wedge-shaped silicon detectors with radial strips, similar to the TID. Rings 1, 2, and 5 are also equipped with stereo modules for reconstruction of the r-coordinate.

Each module of the silicon strip detector has one or two silicon sensors that are glued on carbon fibre (CF) frames together with a ceramic readout hybrid, with a mounting precision of 10 μm. Overall, there are 27 different module designs optimized for different positions in the tracker. The detector modules are mounted on substructures that are, in turn, mounted on the tracker subdetectors.

The TIB is split into two halves for the negative and positive z-coordinates allowing easy insertion into the TOB. The TIB substructures consist of 16 CF half-cylinders, or shells. The mounting accuracy of detector modules on the shells is about 20 μm in the shell plane. The modules are assembled in rows that overlap like roof tiles for better coverage and compensation for the Lorentz angle [3]. An aluminium cooling tube, with 0.3 mm wall thickness and 4×1.5 mm^2 rectangular profile is glued to the mounts of the detector modules. Each row has three modules on one cooling loop and each cooling pipe is connected at the edges of the shells to the circular collector pipe that gives extra rigidity to the whole TIB mechanical structure. The overall positional accuracy of the assembly of all shells is about 500 μm.

The TOB main structure consists of six cylindrical layers supported by four disks, two at the ends and two in the middle of the TOB structure. The disks are made of 2 mm thick CF laminate and are connected by cylinders at the inner and outer diameters. The cylinders are produced from 0.4 mm CF skins glued onto two sides of a 20 mm thick aramid-fibre honeycomb core. The detector modules are mounted on 688 substructures called rods. The rods are inserted into openings on the

2017 JINST 12 P04023

disks, such that each rod is supported by two disks. The accuracy of mounting the rods is about 140 μm in r-φ and 500 μm in z. Each rod has 6 or 12 (for rods with double-sided modules) silicon modules mounted in a row. A 2 mm diameter copper-nickel cooling pipe is attached to the CF frame of the rod. Each module is mounted on the rod with an accuracy of 30 μm by two precision inserts connected to the cooling pipes, and two springs.

Each TEC side consists of nine disks with 16 wedge-shaped substructures on each disk, called petals. Overall there are 144 petals with different layouts, depending on the disk location. The petals are made of CF skins with a honeycomb structure inside. The wedge-shaped detector modules are mounted on the petals with an accuracy of 20 μm using four aluminium inserts that are connected to the cooling pipe. A titanium cooling pipe of about 7 m in length, 3.9 mm in diameter, with 0.25 mm wall thickness is integrated into the petal honeycomb structure and is bent to connect all heat sink inserts. The petals are mounted on the CF disks with a precision of 70 μm. All nine disks of each TEC are connected together with eight CF bars forming a rigid structure. These bars are also used to hold service cables and cooling pipes. The overall accuracy of the disks assembly in the TEC subdetector is about 150 μm in all coordinates.

The main support structure for all tracker subdetectors is the tracker support tube (TST). The TST is a cylinder 5.4 m in length and 2.4 m in diameter made of CF composite. The wall of the TST is made of a 30 mm thick sandwich structure with 2 mm CF skins on both sides, and a 26 mm thick aluminium honeycomb core. The TOB, TECP, and the TECM are supported inside the TST while the TIB and TID are supported by the TOB. The total weight of all subdetectors inside the TST is about 2200 kg, which is distributed on two longitudinal rails connected to the TST with glue and metallic inserts. The TST itself is supported inside the CMS calorimeters by four brackets at each end. According to calculations the maximum deformation of the TST when supporting the assembled tracker is about 0.6 mm. The mounting accuracy of different subdetectors inside the TST is in the range of 1 mm, but the exact position of all subdetectors was measured with an accuracy of 50 μm in an optical survey conducted at the beginning of the detector operation [5]. A possible movement that is beyond the assembly accuracy is considered as a major displacement.

The detector modules, substructures, and subdetectors are joined together using the so-called kinematic connections that constrain the movement in some directions, where the constraints are ensured by the static friction in tension screws. The engineering designs of these connections in the various mechanical structures are different, but the range in all joints suffices to accommodate the expected thermal movement. The fixation points and allowable movements for the subdetectors are indicated in figure 1. In the vertical direction, each subdetector is constrained only by its own weight. The movement in the x-direction is constrained only on one side of the TST. The fixations in the z-coordinate are governed by the assembly procedure. During the assembly, the TOB was first inserted into the TST and fixed in z on one side. Then the TIB and TID halves were inserted into the TOB from each end and fixed against each other in the centre. The TECP and TECM were mounted last, and constrained in z at the internal ends.

Operation of silicon modules exposed to a large radiation fluence requires cooling [3]. The total dissipated power of the readout electronics with a fully powered tracker is about 45 kW. After irradiation the leakage current of the silicon sensors contributes another 10 kW. The heat inside the tracker is evacuated by a monophase liquid-cooling system that uses a fluorocarbon (C_6F_{14}) coolant. Two cooling plants, each with 40 kW capacity, are used for this purpose. Each plant is connected to 90 cooling loops distributed among the different substructures in one half of the tracker.

2017 JINST 12 P04023

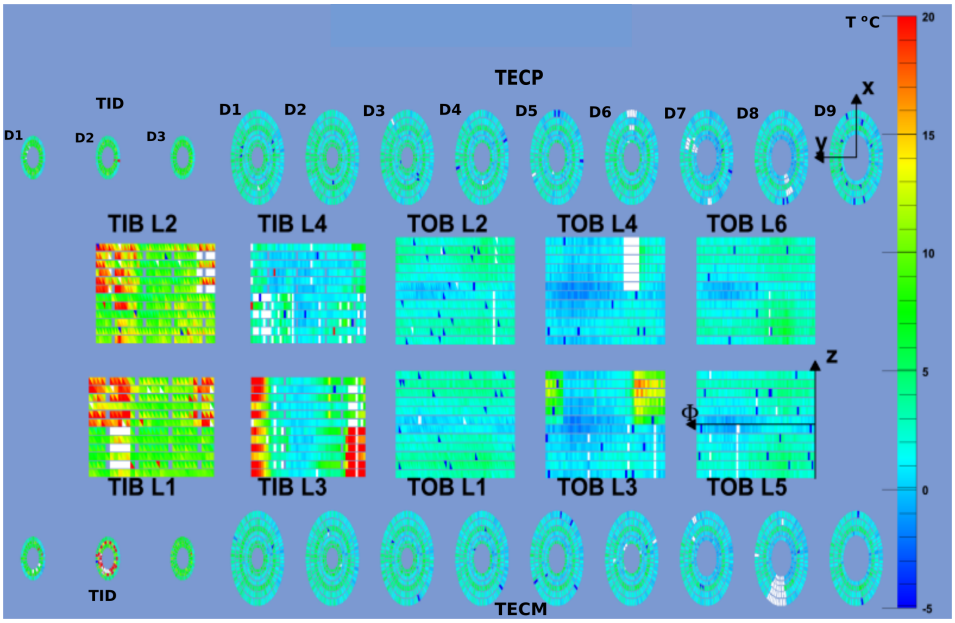

Figure 2. Example of the temperature distribution, shown as a colour palette (°C), measured on silicon sensors in the TIB (L1–L4), TOB layers (L1–L6), and the TEC (D1–D9), TID (D1–D3) disks, with the cooling plant operating at T = −5°C. The white spots correspond to nonoperational detectors, and red spots are the closed cooling loops and bad cooling contacts.

In the first physics run during 2010–2013 (Run 1), the operating temperature of the cooling plant was set to T = +4°C. For Run 2 (2015 onwards), the nominal operating temperature was decreased to −15°C, in order to allow long term operation with increased fluence caused by increased energy of collisions, as well as instantaneous luminosity [3]. The operation at low-temperatures requires a low dew point inside the tracker. The whole tracker volume is separated from the TST inner wall by a thermal screen, apart from the points at which the subdetectors are attached to the rails that remain at ambient temperature. The thermal screen has cooling elements inside and heating elements outside the tracker volume, thus acting as a thermal barrier that prevents condensation. The inner tracker volume of about 25 m^3 is constantly flushed with dry air or nitrogen at a rate of about 20 m^3/hour, such that the dew point in the CMS cavern of about +10°C is reduced to below −40°C inside the tracker volume. All service cables and cooling pipes leave the subsystem at the tracker bulkheads, which are also isolated by the thermal screen and flushed with dry gas at a higher rate of about 150 m^3/hour.

The temperature of the different mechanical structures inside the tracker depends on the distribution of heat sources and heat sinks. The temperature and humidity inside the tracker are monitored by dedicated sensors mounted directly on readout hybrids, silicon sensors, and mechanical structures, distributed throughout the detector volume. The nonuniformity of heat dissipation and heat removal results in significant temperature variations inside the tracker even in thermal equilibrium. Large temperature gradients are observed near the readout hybrids, the cooling tubes and the mounting connections. Figure 2 shows the temperature measured on silicon sensors in different subdetectors running with a cooling plant at operating temperature of −5°C.

2017 JINST 12 P04023

The white areas represent non-operational detectors, which comprise about 2.5% of the total area. The red (hot) spots are five cooling loops (three in the TIB, and one in the TOB and the TID) that are closed because of leaks and bad cooling contacts (layers L1, and L2 in the TIB).

A local change of temperature naturally causes an increase in the nonuniformity. For example, the powering of the module readout electronics rapidly increases the local temperature by about 15°C and it takes about one hour to stabilize the temperature in the tracker volume. Cooling down from the ambient temperature of about +15°C to +4°C takes about 3 hours before stabilization of temperature.

3 The laser alignment system

The initial purpose of the LAS was to measure relative positions of the tracker subdetectors with an accuracy of about 10 μm and the absolute position with an accuracy of 100 μm. The large temperature variations expected in the tracker determined the design concept and components for the LAS; the components had to be light, radiation hard, operational in a high magnetic field, and capable of sustaining large temperature variations.

The LAS has 40 infrared laser beams that illuminate the silicon strip modules in the outer layer of the TIB, inner layer of the TOB, and in rings 4 and 6 of the TECs, as shown in figure 3. The LAS uses the same detector modules that are used for particle detection. Laser pulses are triggered during the 3 μs orbit gap corresponding to 119 missing bunches in the LHC beam structure that has an orbit time of 89 μs, thus not interfering with collisions [2]. The laser beams are split into two sets. Eight beams are used for global alignment of the TIB, TOB, and the TECs relative to each other. The other 32 beams are used to internally align the disks in the TECP and TECM subdetectors. The pixel and the TID subdetectors are not included in the LAS monitoring. Since the tracker has approximate axial symmetry, the beams are distributed rather uniformly in the φ-direction, with the exact position defined by the mechanical layout. Each laser beam used for global alignment illuminates six modules in the TIB, six modules in the TOB, and five modules in each of the TECP and TECM subdetectors. Each laser beam for the internal TEC alignment traverses nine modules in each TEC subdetector.

The LAS components include laser diodes, depolarizers, optical fibres, beam splitters, alignment tubes, mirrors, and specially treated silicon sensors. The laser diodes QFLD-1060-50S produced by QPhotonics have a wavelength of $\lambda = 1075 \pm 3.5$ nm and a maximum optical power of 50 mW. The attenuation length of this laser light in silicon is 10 cm at 0°C and decreases by 1%/°C with increasing temperature. The light output of each laser is regulated by an operating current in the range of 0–240 mA and is optimized as discussed below. The lasers operate in pulsed mode with a pulse width of 50 ns. The spectral bandwidth of the lasers is $\Delta\lambda = 2.4 \pm 0.9$ nm, which defines the coherence length $\lambda^2/\Delta\lambda \approx 480\,\mu$m. A coherence length larger than $2d{\cdot}n_{Si}$ (where d is the silicon thickness of 320–500 μm and $n_{Si} \approx 3.5$ is the silicon refractive index) would result in interference of the laser light reflected on the front- and back-side of the sensor, hence degrading the laser beam profile. Because of the harsh radiation conditions in the CMS detector cavern, the laser diodes are located in the outer underground service area. The light is distributed to different subdetectors via special 0.125 mm diameter Corning monomode optical fibres.

The light from the lasers is directed towards different subdetectors using beam splitters (BS) that divide the light into back-to-back beams, as shown in figure 3. For the global alignment the

2017 JINST 12 P04023

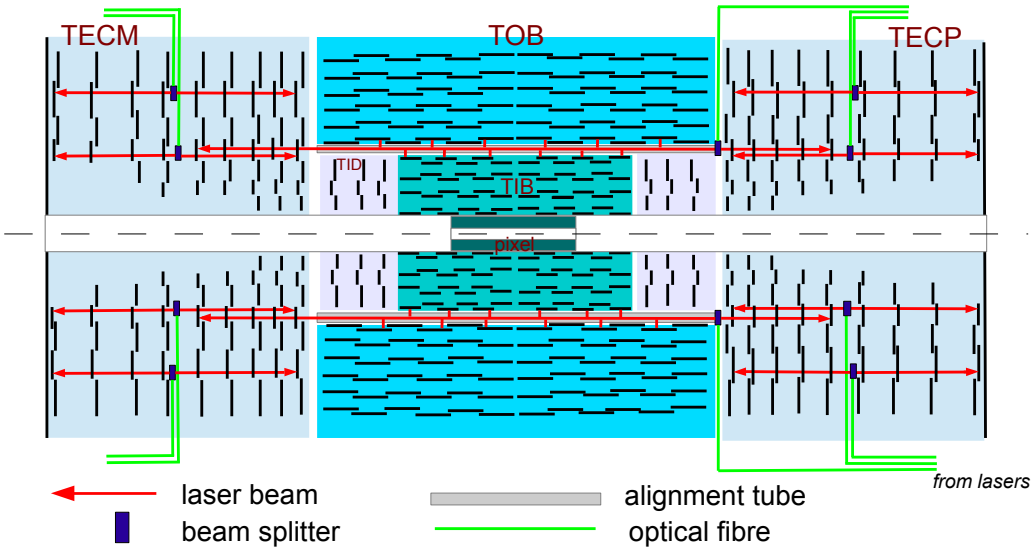

Figure 3. Distribution of the laser beams in the CMS tracker. The eight laser beams inside the alignment tubes are used for the global alignment of TOB, TIB, and TEC subdetectors. The 32 laser beams in the TECs are used for the internal alignment of TEC disks.

eight beam splitters for the eight laser beams are mounted between the TOB and TECP. For the internal TEC alignment, 32 BS are located on disk 6 in both TECP and TECM. The principle of operation of the beam splitter is based on polarization using a λ-plate, as shown in figure 4. The incoming beam, consisting of both s- (perpendicular to the plane of incidence) and p- (parallel) polarizations, is collimated onto a 45° inclined surface with a special coating, from which the s-polarized part of the laser light is completely reflected. The p-fraction continues, traversing a $\lambda/4$-plate and converting into right circular polarization. The light is reflected by a mirror after the plate and changes polarization to left circular. After a second traversal of the $\lambda/4$-plate, the left circularly polarized light becomes s-polarized and is completely reflected onto the other side of the 45° inclined surface. At the end, there are two parallel back-to-back beams with s-polarization in the z-direction. The important characteristic of the splitter is the variation of collinearity as a function of the beam spot position. For all BS, the collinearity is measured to be less than 50 μrad for the −25 to +25°C temperature range. Since the laser light is polarized, splitting based on a λ-plate requires depolarization. The depolarizers (produced by Phoenix Photonics) are located in the service area just after the laser diodes and before the optical fibres.

Dedicated alignment tubes (AT) between the TIB and TOB are used to hold the BS and semitransparent mirrors that reflect light towards TOB and TIB detector modules, as shown in figure 4. The eight laser beams between TOB and TIB pass through the AT and continue to the TECM disks. The AT are made from 16 mm diameter aluminium and are integrated into the TOB support wheels. The mirrors mounted inside the AT are glass plates that reflect about 5% of the light intensity perpendicular to the beam (S_1). The antireflective coating on the back side of the mirror and the s-polarization of the laser light after the beam splitter prevent the second reflection (S_2). The mounting accuracy of each AT is about 100 μm, but with temperature variations the aluminium can expand by about 0.5 mm/m/20°C. Although this expansion is mostly along the z-direction, the

2017 JINST 12 P04023

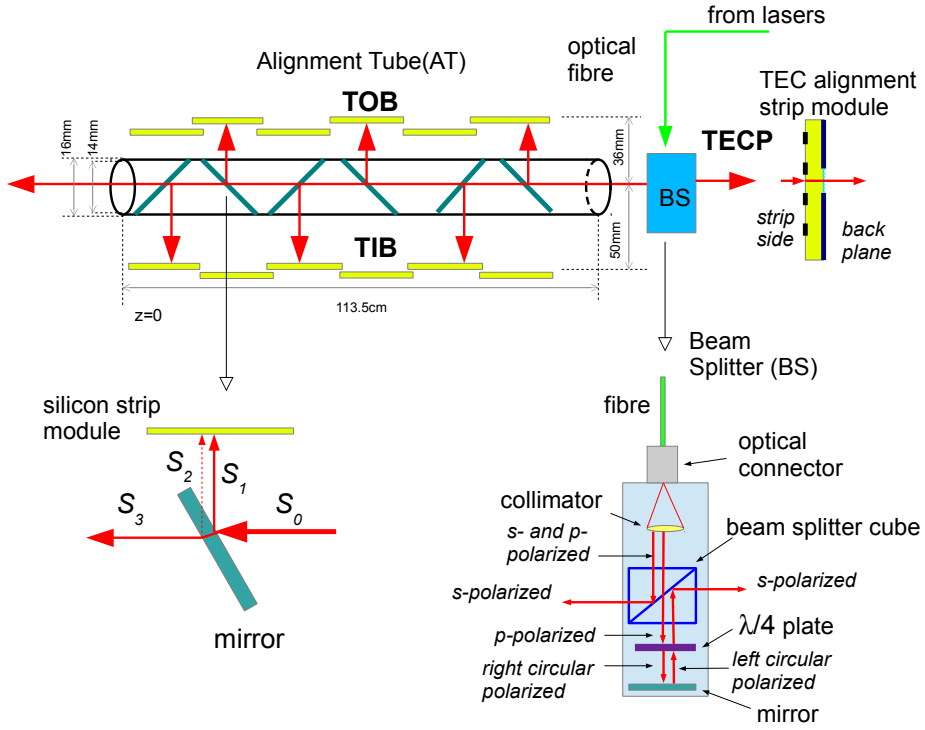

Figure 4. The LAS components: alignment tube, mirror, and beam splitter.

movement can affect the orientation of the BS and therefore the direction of the laser beams. Such variations are taken into account in the LAS reconstruction procedure, as discussed below.

Overall the laser beams hit 449 silicon sensors, with a strip pitch varying from 120 μm in the TIB to 156 μm in the TEC detector modules. The 48 TIB and 48 TOB sensors that are used by the LAS are standard ones, and are illuminated on the strip side. On the other hand, 353 TEC sensors had to be modified to allow the passage of laser light. For the standard sensors, the backplane is covered with aluminium coating and is therefore not transparent to the laser light. For the TEC modules this coating was removed in a 10 mm diameter circular area of the anticipated laser spot position. In addition, an antireflective coating was applied in this area in order to improve the transparency. An attempt also to coat the strip sides resulted in changes of the silicon sensor electrical properties and was therefore abandoned.

Since the detector modules illuminated by lasers are also used for particle tracking, their readout electronics is exactly the same as for other silicon strip modules in the tracker [3]. The signal from the silicon strips is processed in the analogue pipeline readout chip (APV25) [2], and transferred to the data acquisition (DAQ) by optical fibres. The analogue signal from the APV25 chip is digitized by the analogue-to-digital converters (ADC) located in the CMS underground service cavern, and is processed further similarly to physics data. The LAS-specific electronics include a trigger board that is synchronized with the CMS trigger system and the 40 laser drivers.

The trigger delay for each laser driver is tuned individually to ensure that the laser signals arrive at the detector module properly synchronized with the CMS readout sequence. The laser intensity is also optimized individually to account for losses in the optical components and attenuation in the

2017 JINST 12 P04023

TEC silicon sensors. The amplitude and time settings for each laser driver are defined in a special calibration run, during which the laser intensity and delays are scanned in small steps. There are five settings available for each laser, to be shared between up to 22 detector modules illuminated by the same laser beam. This results in some variations of the laser signal amplitude in different detectors.

One regular LAS acquisition step consists of 2000 triggers. The first 1000 triggers are optimized for the global alignment, whilst the other 1000 triggers are used for the internal alignment of both TECs. The lasers are triggered with five different settings delivering 200 suitable laser shots for each illuminated module. The signal-to-noise ratio for the 200 accumulated pulses is above 20, which is similar to the signal from particle tracks. The lasers are triggered in the orbit gap of every hundredth LHC beam cycle, corresponding to a rate of 100 Hz and resulting in about 20 s per acquisition step. During normal data taking the acquisition interval was set to 5 minutes to achieve a good compromise between the time resolution of the LAS alignment and the stored data volume. Since the LAS electronics is deeply integrated into the CMS data acquisition, it works only when the tracker and the DAQ are operational and configured for a global physics run. Intervals between the runs, periods of testing, and technical stops are not covered by the LAS measurements.

4 Tracker alignment

The general tracker alignment procedure reflects the mechanical structure of the detector. The largest alignable objects are the tracker subdetectors, and the smallest ones are the silicon sensors. Each alignable object is considered as an independent and mechanically rigid body that can move and rotate in six degrees of freedom: three offsets $(\Delta x, \Delta y, \Delta z)$ and three rotations (Rx, Ry, Rz) around the axes, as shown in figure 1.

The alignment procedures used with particle tracks and the LAS data differ somewhat. In the LAS, the assembly accuracy and the mechanical stability of the optical components are about 100 μm, limiting the accuracy of absolute alignment to about 50 μm [9]. Relative displacements with respect to a reference position can be monitored using LAS data with a much better precision of a few μm. However, the limited number of laser beams only allows the reconstruction of the relative displacement of large structures, such as the TOB, TIB, and the TECs, using some assumptions discussed below.

The alignment with tracks does not have the aforementioned limitations [6]. The cosmic ray muon and collision tracks are copiously measured in CMS and are used to derive the absolute alignment parameters in the CMS coordinate system down to individual detector modules. The number and distribution of tracks define the time interval and the accuracy of different alignment parameters in the track-based alignment. For example, the alignment of large structures, similar to the alignment with LAS, can be performed after a few hours of data taking. In the following we describe some aspects of the alignment procedures using the LAS data and particle tracks.

4.1 Alignment with the laser system

The LAS alignment procedure is based on a few assumptions. First, we assume that the LAS can measure only relative displacements of the laser beam profile with respect to some reference position. In this study all displacements are derived with respect to the TOB position because the TOB holds the alignment tubes and is directly connected to the TST. The offsets of laser

2017 JINST 12 P04023

beam profiles from the reference positions are thus used to calculate the variations of alignment parameters, not their absolute values. The relative alignment assumes that all tracker components, including the LAS elements, can move.

The second assumption concerns the definition of alignable objects and their parameters. The laser beams used for the global alignment allow the reconstruction of displacements of the TOB and TIB in Δx, Δy, and rotations Rx, Ry, Rz, while movement along the z-axis is not measured in the barrel due to the orientation of strips along z. The same laser beams in the TECP and TECM are used to reconstruct Δx, Δy and Rz, while other parameters are not constrained due to the radial orientation of the TEC strips. In the LAS alignment procedure, each subdetector is considered as a rigid body and all deviations from this model are treated as systematic uncertainties.

Further, it is also assumed that the orientation of the laser beams can vary, for example, due to temperature variation in the alignment tube leading to small rotations of the beam splitters. The direction of each ith laser beam is parameterized by the two parameters: the offset α_i, and slope β_i in the φ-z plane. These laser beam parameters are estimated from the LAS measurements together with other alignment parameters in one global fit. Note that the laser beams passing through the mirrors or through the silicon sensors may have some kinks, but these kinks are independent of the beam orientation. The assumption of the straightness of the laser beams implies that all of the optical components of the LAS have flat surfaces near the laser beam spot, such that small displacements of the LAS components do not affect the alignment parameters.

Under the above assumptions the LAS alignment procedure has two main steps: reconstruction of laser beam profiles and evaluation of alignment parameters. The laser profile is defined as an accumulated amplitude in ADC counts versus strip number within a module after 200 laser shots. The profile depends on the laser intensity, the silicon strip pitch and the width of the laser beam spot after propagation of laser light through beam splitters, mirrors, and silicon sensors (for TECs). Figure 5 shows beam profiles for different subdetectors obtained in two acquisition steps. The position of the laser beam spot is obtained from the intersection of the linear extrapolations of the profile at its half-maximum. The strip pitches for the illuminated TIB, TOB, and TEC modules are the 120, 122, and 128 μm respectively. For the TOB and TIB the profiles are Gaussian-like, while for the TEC detectors, where the light passes through the silicon, the profiles show a diffraction pattern caused by reflections inside the silicon sensor.

The second step is the reconstruction of the alignment parameters with respect to the reference position in each illuminated module. The displacements of the beam position ψ^j in detector module j with respect to the reference position ψ^j_{ref} are given by $\delta^j = \psi^j - \psi^j_{\text{ref}}$. These displacements δ^j are inputs to the $\chi^2 = \Sigma(\delta^j - \phi^j(\vec{p}))^2/\sigma_j^2$, where $\phi(\vec{p})$ are the predicted displacements depending on the fit parameters $\vec{p}$: α_i, β_i, Δx, Δy, Rx, Ry, Rz. For the χ^2 minimization, the $\partial\chi^2/\partial p_k$ derivatives are linearized using the small-angle approximation. The system of linear equations is solved analytically using matrix inversion with respect to the parameters p_k. The LAS alignment procedure is flexible; some measurements or all measurements from a specific laser beam can be excluded from the fit, and the number of fit parameters can be varied, for example excluding rotations or offsets. These features were used to check the stability of the alignment procedure and systematic uncertainties. The results from different fit configurations agree within 10 μm.

The stability of the alignment parameters reconstructed with the LAS has been studied during periods (of a few weeks) of operation at a fixed temperature where we expect no real movements of

2017 JINST 12 P04023

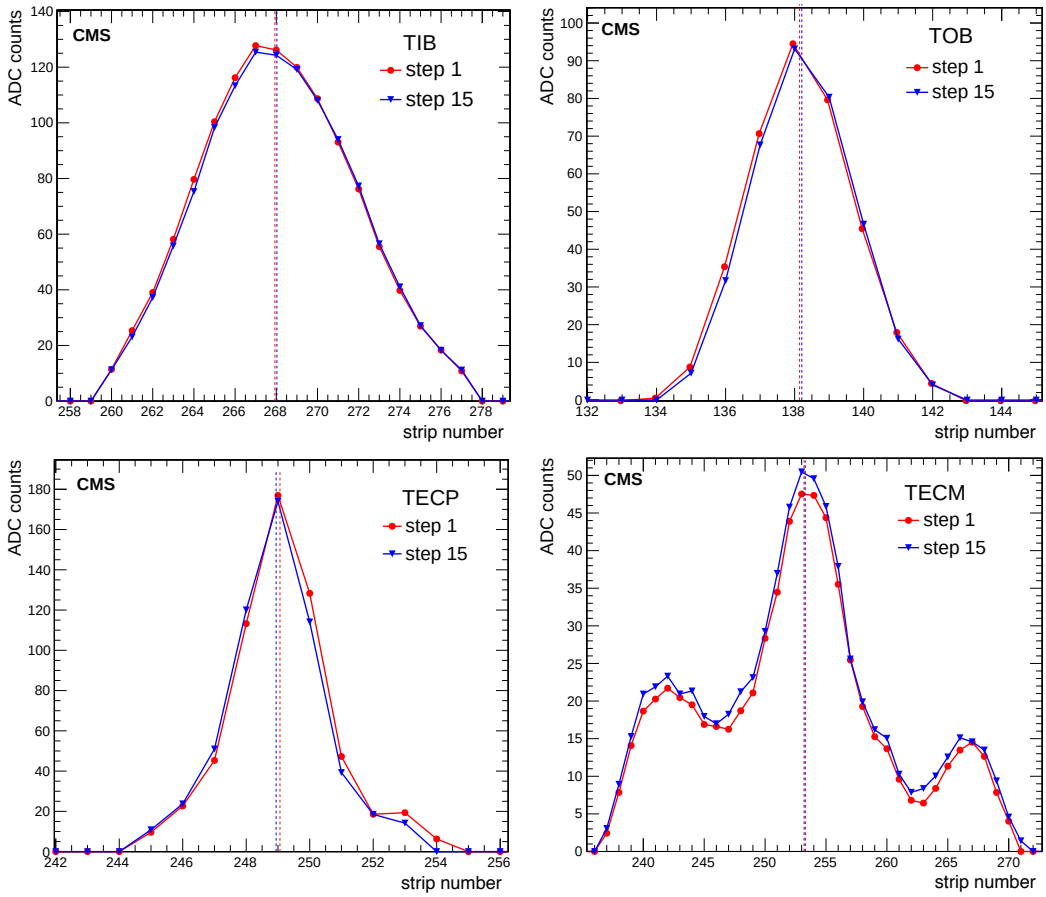

Figure 5. Examples of laser beam profiles (accumulated amplitude in ADC counts for 200 laser shots vs. strip number) in the TIB, TOB, TECP, and TECM modules, obtained in two different acquisition steps. The vertical dashed line shows the reconstructed laser spot position. In the TECM, two lower diffractive peaks are visible as mentioned in the text.

the tracker components. The stability is defined as one standard deviation of the distribution of each alignment parameter. A summary of the LAS alignment parameters and their stability is presented in table 1. The best stability of about 1 μm is obtained for the relative Δx and Δy displacements of the TIB. For the TECM profiles the stability worsens to 2–3 μm due to larger distortion of the laser beam after passing through many mirrors.

Table 1. Stability of alignment parameters using LAS measurements obtained during periods of operation at a fixed temperature.

	Δx [μm]	Δy [μm]	Rx [μrad]	Ry [μrad]	Rz [μrad]
TIB	0.9	0.9	1.7	1.6	1.1
TECP	1.4	1.4	—	—	1.7
TECM	2.2	2.5	—	—	2.9

2017 JINST 12 P04023

4.2 Alignment with particle tracks

A detailed description of tracker alignment with tracks can be found in numerous publications, e.g. in ref. [6] and references therein. One of the track-based alignment algorithms used in CMS is MILLEPEDE II [8]. The algorithm simultaneously reconstructs the track parameters $\vec{x}$ for each event and the alignment parameters $\vec{p}$ for each alignable object, and involves two steps. In the first step the $\partial f/\partial x_i$ and $\partial f/\partial p_k$ derivatives of the track model $f(\vec{x}, \vec{p})$ with respect to the track and alignment parameters are calculated. These derivatives are stored in a matrix with the size of $(n_{\text{tracks}} n_{\text{trackpar}} + n_{\text{algnpar}})^2$, where n_{tracks} is the number of selected tracks, n_{trackpar} is the number of individual track parameters (four for propagation without magnetic field and five for propagation in the field), n_{algnpar} is the number of alignment parameters. Then the corresponding system of linear equations is reduced in size using block matrix algebra and solved numerically [6].

The phase-space of particle tracks defines the sensitivity of the track-based alignment procedure to a particular alignment parameter. Two types of tracks can be used; tracks from collisions that originate in the detector centre, and tracks from cosmic rays that can cross the detector away from the interaction point. For the 2012 period, about 15×10^6 collision tracks and 4×10^6 cosmic ray tracks were used for the alignment. The track samples are split into separate periods in time that are used to calculate the alignment parameters for all detector modules. The intervals should be chosen such that, within each period, the operations do not vary significantly, but at the same time should provide sufficient statistics for the MILLEPEDE procedure. Usually, each interval corresponds to a few months of stable operation. The reconstruction accuracy of different alignment parameters in the track-based alignment depends on the number of selected tracks and on the location of the detector modules [6].

5 Tracker mechanical stability

The tracker mechanical structures have a hierarchy, and can be grouped as follows: subdetectors (TIB, TOB, TECs), substructures (shells, rods, petals), and individual detector modules. All these components can potentially move for different reasons and over different time scales. We distinguish between short-term variations, which occur over an interval of a few hours, and long-term variations, which occur over a period of a few days or months.

Temperature variation is expected to be the main source of movement in the tracker during physics operation. The thermal expansion of the CF composite used in the support structures is about 2.6×10^{-6}/°C. For the 2.4 m long TOB this would result in displacements of about 60 μm for ΔT = 10°C. Since the mechanical design of the tracker allows for thermal expansion, the temperature-related movements should be elastic, that is, the positions are restored when the temperature is restored to its original value. However, this process can be disrupted by the uncontrollable static friction in kinematic joints and the thermal expansion of power cables, cooling pipes, etc. that are integrated into the structures of the tracker. Many thermal cycles of the tracker can thus result in some nonelastic displacements and non-rigid body deformations.

The release of intrinsic stresses produced during assembly is another source of movement that can happen occasionally or be initiated by the temperature variations. Variations of the magnetic field, intervention in the CMS cavern and mechanical work during technical stops can also cause the

2017 JINST 12 P04023

movement of some CMS components and affect the tracker alignment. These movements, as well as nonelastic movements and deformations, are difficult to simulate in finite-element method models, thus making experimental measurements indispensable for validation of the mechanical design.

5.1 Long-term stability

The long-term stability of global alignment parameters reconstructed with the LAS data in the years 2011–2013 is shown in figure 6 and in more detail in figures 7–10. The alignment parameters of the TIB and TECs are calculated with respect to the TOB. Each point in the plots corresponds to one LAS acquisition step with an interval of 5 minutes, and the uncertainties are from the LAS global fit. Different parameters can overlap in figure 6, but the range of variations during the whole period is clearly visible. The operating temperature of the cooling plants was set to +4°C throughout the operation period, resulting in a temperature of about +6°C in the return pipe, which is shown as the black line in the figures. The positive spikes in the temperature correspond to the occasional power down of the cooling plants, and the small negative spikes of about 2°C are due to switching off the low-voltage supplies to the detector modules. The stability of the internal TEC alignment parameters is similar and is not discussed in this paper.

The whole period of 2011–2013 can be split into different parts. Periods with no LAS data are due to either nonoperational global CMS DAQ or nonoperational tracker. Loss of data resulting from LAS problems was below 1% and related to the occasional powering down of the LAS electronics in the service area.

Most of the LAS data were collected during periods of operation at stable temperature inside the tracker volume. The alignment parameters of the TIB and TEC are remarkably stable; all variations in displacements are within $\pm 10\,\mu$m for the TIB, $\pm 20\,\mu$m for the TECP, and $\pm 30\,\mu$m for the TECM. The expanded view of some typical parts shown in figure 6 can be seen in figure 7, for example the periods of operation at stable temperature for the TIB and TECM are presented in the upper plots.

Stable operation is often interrupted by transient periods when alignment parameters change by more than $10\,\mu$m (or $10\,\mu$rad) for TIB and $30\,\mu$m ($30\,\mu$rad) for TECs during an interval of a few hours. All these periods are associated with temperature variations. The temperature can change rapidly due to occasional trips of cooling plants or, more often, due to a power trip affecting some detector modules. The powering down of the low voltages of the readout hybrids reduces the temperature locally by about 15°C. The actual temperature variations depend upon how fast the cooling or voltages are restored, while the observed variations of the alignment parameters depend on when the LAS acquisition was restarted. The bottom left plot in figure 7 shows an example of the evolution of the TIB alignment parameters after a power trip, affecting the whole tracker. Power to the tracker was restored and the LAS data acquisition restarted after 30 minutes, thus the movement during these 30 minutes was not recorded. The observed evolution of the alignment parameters follows the temperature stabilization in the tracker volume, which takes about an hour. Similar effects can be observed during the powerdown of the cooling plants; in this case the expected temperature variations and, therefore, the observed displacements are bigger, as can be seen in the bottom-right plot in figure 7. The periods with large transient variations of alignment parameters are excluded from physics analysis.

The long periods of data taking are separated by a few technical stops when the whole CMS detector is powered down. During this time the temperature in the tracker is not controlled and is

2017 JINST 12 P04023

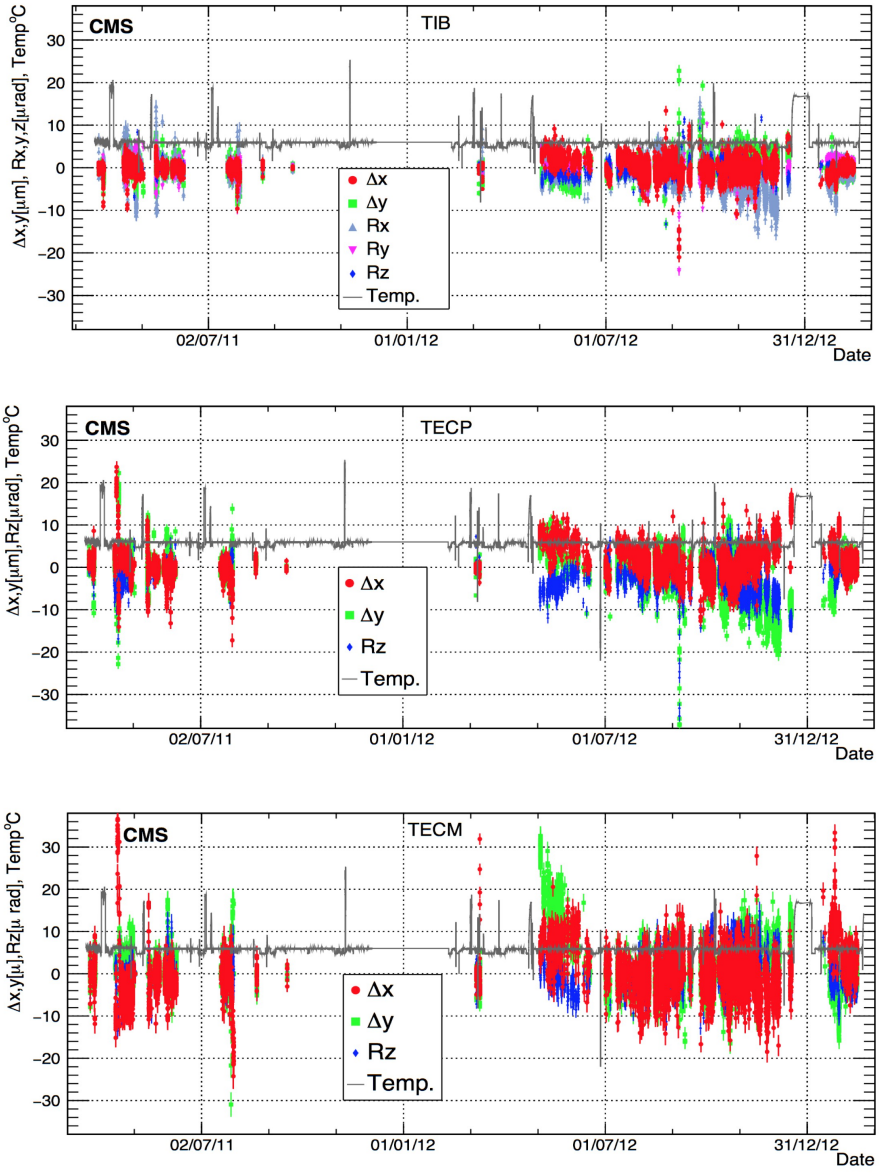

Figure 6. Stability of TIB, TECP, and TECM alignment parameters during 2011–2013 data taking. The black line is the temperature of the cooling liquid in the return circuit.

close to the ambient temperature in the detector cavern. At the same time some mechanical work and intervention to the CMS detector can take place. Hence, after each of these technical stops a new reference position is used in the LAS alignment procedure described above.

The long-term evolution of the alignment parameters calculated with the LAS data is compared with the results obtained from the alignment with particle tracks in figures 8–10. The alignment parameters for the 2012 period are calculated for ten intervals that correspond to the LAS periods with new reference positions. The MILLEPEDE alignment configuration was similar to the configuration for the LAS measurements, that is, the TOB position was fixed, and the TIB and TEC

2017 JINST 12 P04023

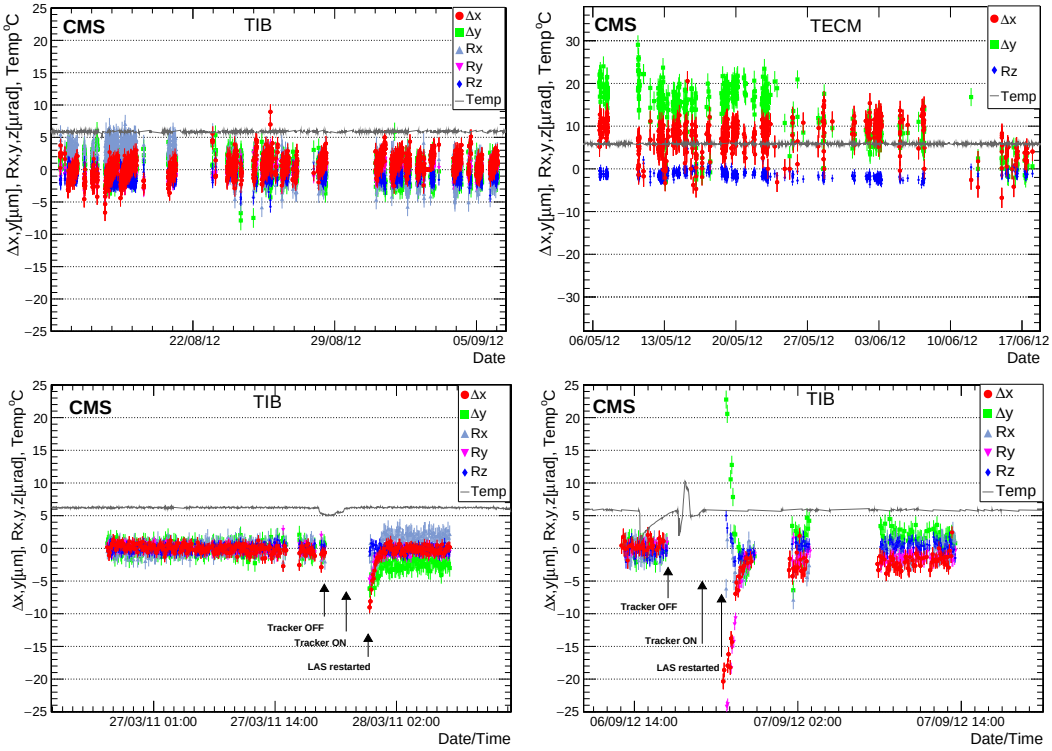

Figure 7. Expanded view of the tracker alignment stability for selected time intervals. Upper left: TIB parameters during weeks of operation at stable temperature. Upper right: variations of TECM parameters at stable temperature. Bottom left: variations of TIB parameters after a power trip. Bottom right: TIB parameters after cooling plant shutdown and recovery.

subdetectors were considered as rigid bodies that can move with the same degrees of freedom as used in the LAS. Since MILLEPEDE delivers absolute alignment parameters based on measurements in many detector modules, whilst the LAS measures relative displacements and only for the illuminated modules, some differences between the parameters derived with the two different methods are expected. However the variations of the parameters in both measurements are similar and are within 30 μm (or 30 μrad), confirming the long-term mechanical stability of large structures of the tracker. The displacements below 30 μm can have different origins; for example they could be related to deformations of other components of the CMS detector. Since all observed large transient variations in the alignment parameters coincide with the variations of the temperature in the tracker volume, a dedicated thermal model can be used in the future to predict displacements using solely the temperature measurements.

5.2 Stability during temperature variations

Large variations of alignment parameters correlated with the temperature were studied during the long shutdown of the LHC in 2013. The tracker alignment parameters were reconstructed when the tracker was cooled down from a target temperature of +4 to −10°C, and then warmed up again. The evaluation of the TIB alignment parameters during temperature transitions from +4 to −10°C in steps of $\Delta T = 5$°C is shown in figure 11. The periods without data are due to other CMS

2017 JINST 12 P04023

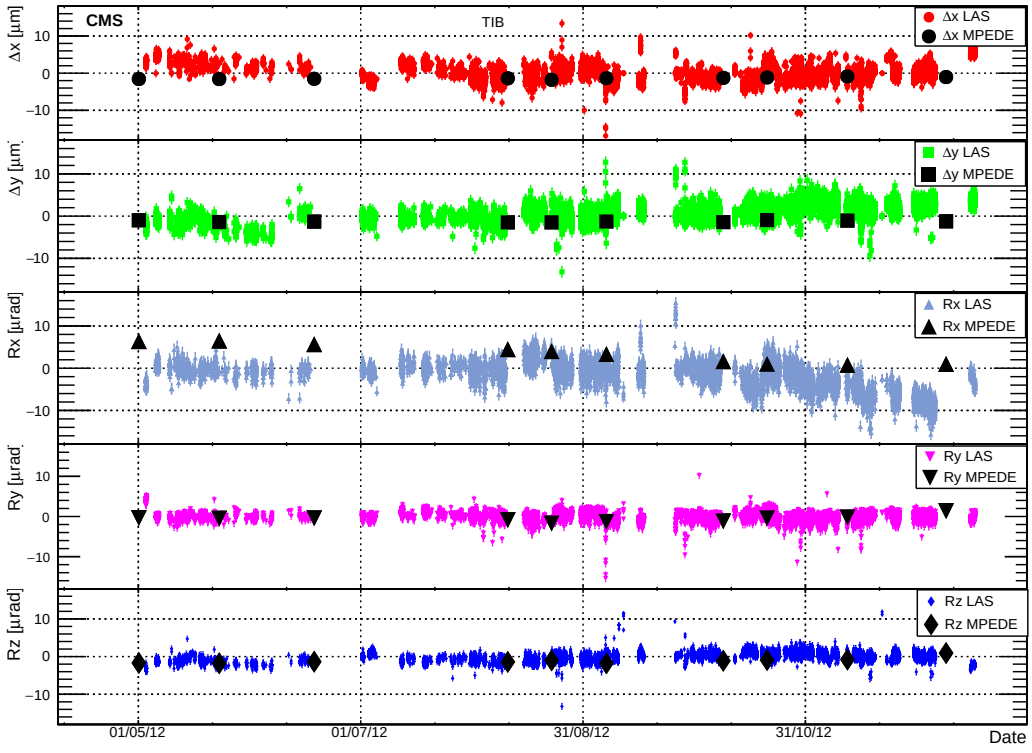

Figure 8. Comparison of the TIB alignment parameters reconstructed with LAS data and calculated with MILLEPEDE from measured particle tracks.

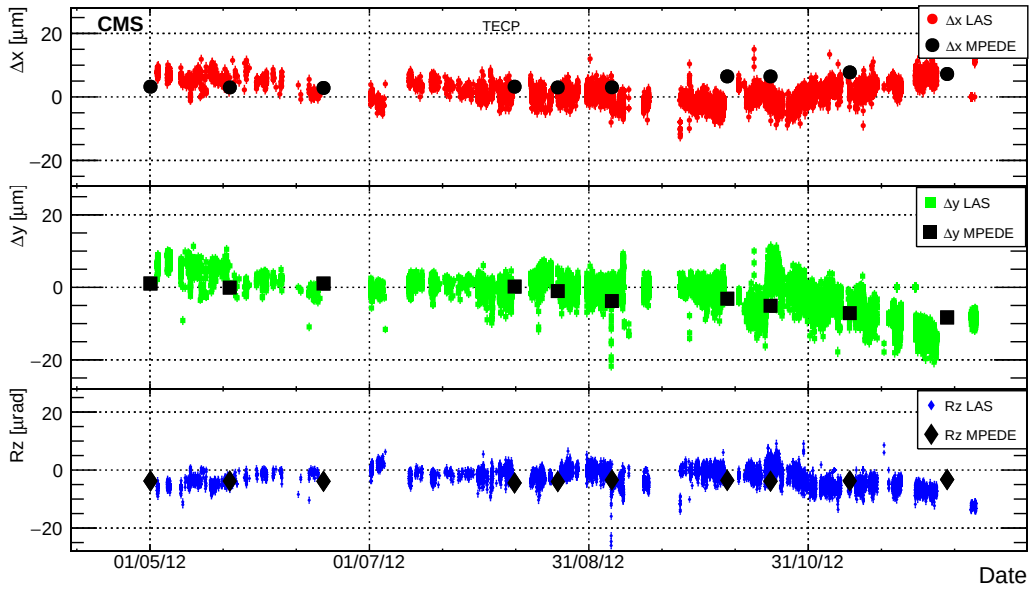

Figure 9. Comparison of TECP alignment parameters measured with LAS and calculated with MILLEPEDE from measured particle tracks.

2017 JINST 12 P04023

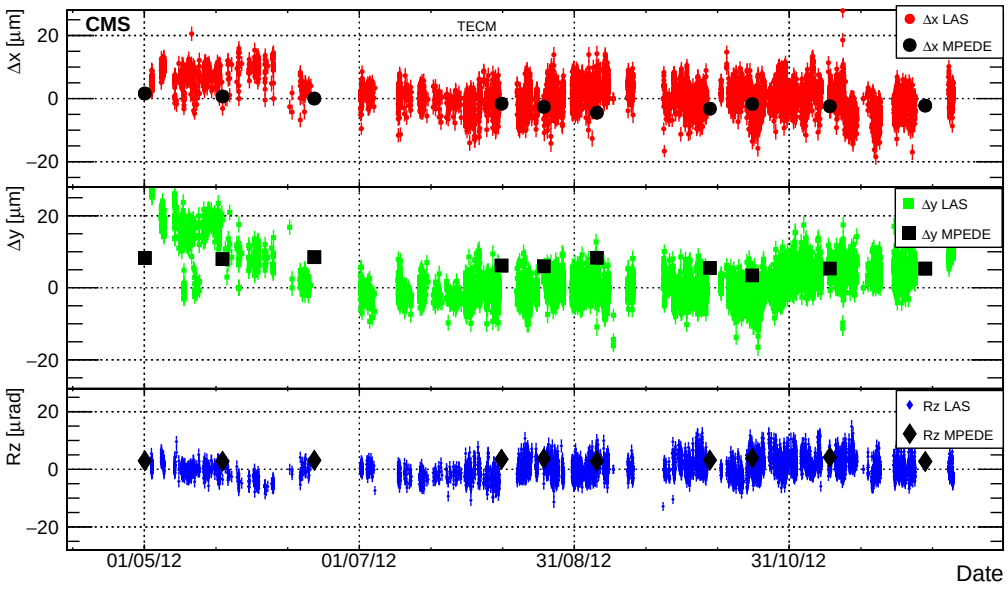

Figure 10. Comparison of TECM alignment parameters measured with LAS and calculated with MILLEPEDE from measured particle tracks.

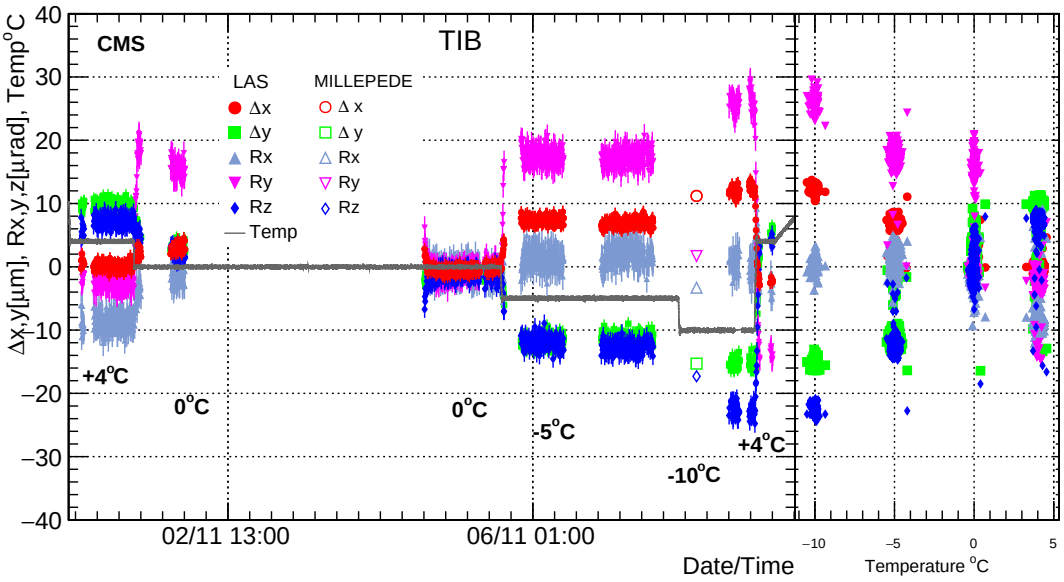

Figure 11. Evolution of the TIB alignment parameters calculated with LAS during tracker thermo-cycling $+4 \rightarrow 0 \rightarrow -5 \rightarrow -10 \rightarrow +4°C$. The MILLEPEDE points from cosmic ray muons are shown as open markers for the $0 \rightarrow -10°C$ transition. The right-hand side of the figure groups the data at each different temperature, so that the correlation between alignment parameter values and operating temperature can be more easily distinguished.

commissioning activities that prevented LAS operation. For all cooldown transitions the pattern of movements is rather similar; the parameters change monotonically with temperature. When cooled by $\Delta T = 5°C$, the TIB Δx increases by about 5 μm, Δy decreases by 10 μm, and the detector rotates around the y-coordinate by about 20 μrad. This corresponds to temperature-related displacements

2017 JINST 12 P04023

of 1–2 μm/°C. Some relaxation of the Ry rotation is observed for the long period at 0°C. Warming up eliminates most of the variations immediately, with some remaining residuals of about 20 μm that were not followed up in this test due to other CMS activities.

The alignment parameters were also calculated with MILLEPEDE using tracks from cosmic ray muons, as shown in figure 11. About 1.6×10^3 and 4×10^3 cosmic ray tracks were recorded for the 0°C and −10°C cooling steps, respectively. The MILLEPEDE configuration was similar to the long-term stability measurements described in the previous section. The reference position was taken at 0°C. Despite low statistics, both measurements are in reasonable agreement for all alignment parameters except for the Ry rotation. This rotation was weakly constrained by cosmic ray tracks because during the shutdown only the central part of the muon system was used for the trigger.

6 Summary

The mechanical stability of the CMS tracker was successfully monitored during the period 2011–2013 using a dedicated laser alignment system and particle tracks from collisions and cosmic ray muons. During operation at stable temperatures, the variations of alignment parameters were less than 30 μm. Larger changes were found to be related to temperature variations caused by the occasional power trip of some modules or of the cooling plant. These temperature-related displacements of the tracker subdetectors are of the order of 2 μm/°C and are largely eliminated when the temperature is restored to its original value.

The results presented in this study have been crucial for the CMS tracker operation in cold conditions. They have established that major mechanical displacements do not take place, and have shown the importance of monitoring the temperature within the detector volume. The observed behaviour of the tracker components under various conditions reported here provides guidance for future upgrades of the CMS tracking system.

Acknowledgments

We congratulate our colleagues in the CERN accelerator departments for the excellent performance of the LHC and thank the technical and administrative staffs at CERN and at other CMS institutes for their contributions to the success of the CMS effort. In addition, we gratefully acknowledge the computing centres and personnel of the Worldwide LHC Computing Grid for delivering so effectively the computing infrastructure essential to our analyses. Finally, we acknowledge the enduring support for the construction and operation of the LHC and the CMS detector provided by the following funding agencies: the Austrian Federal Ministry of Science, Research and Economy and the Austrian Science Fund; the Belgian Fonds de la Recherche Scientifique, and Fonds voor Wetenschappelijk Onderzoek; the Brazilian Funding Agencies (CNPq, CAPES, FAPERJ, and FAPESP); the Bulgarian Ministry of Education and Science; CERN; the Chinese Academy of Sciences, Ministry of Science and Technology, and National Natural Science Foundation of China; the Colombian Funding Agency (COLCIENCIAS); the Croatian Ministry of Science, Education and Sport, and the Croatian Science Foundation; the Research Promotion Foundation, Cyprus; the Secretariat for Higher Education, Science, Technology and Innovation, Ecuador; the Ministry of Education and Research, Estonian Research Council via IUT23-4 and IUT23-6 and European Regional Development Fund, Estonia; the Academy of Finland, Finnish Ministry of Education and

2017 JINST 12 P04023

Culture, and Helsinki Institute of Physics; the Institut National de Physique Nucléaire et de Physique des Particules / CNRS, and Commissariat à l'Énergie Atomique et aux Énergies Alternatives / CEA, France; the Bundesministerium für Bildung und Forschung, Deutsche Forschungsgemeinschaft, and Helmholtz-Gemeinschaft Deutscher Forschungszentren, Germany; the General Secretariat for Research and Technology, Greece; the National Scientific Research Foundation, and National Innovation Office, Hungary; the Department of Atomic Energy and the Department of Science and Technology, India; the Institute for Studies in Theoretical Physics and Mathematics, Iran; the Science Foundation, Ireland; the Istituto Nazionale di Fisica Nucleare, Italy; the Ministry of Science, ICT and Future Planning, and National Research Foundation (NRF), Republic of Korea; the Lithuanian Academy of Sciences; the Ministry of Education, and University of Malaya (Malaysia); the Mexican Funding Agencies (BUAP, CINVESTAV, CONACYT, LNS, SEP, and UASLP-FAI); the Ministry of Business, Innovation and Employment, New Zealand; the Pakistan Atomic Energy Commission; the Ministry of Science and Higher Education and the National Science Centre, Poland; the Fundação para a Ciência e a Tecnologia, Portugal; JINR, Dubna; the Ministry of Education and Science of the Russian Federation, the Federal Agency of Atomic Energy of the Russian Federation, Russian Academy of Sciences, the Russian Foundation for Basic Research and the Russian Competitiveness Program of NRNU MEPhI (M.H.U.); the Ministry of Education, Science and Technological Development of Serbia; the Secretaría de Estado de Investigación, Desarrollo e Innovación and Programa Consolider-Ingenio 2010, Spain; the Swiss Funding Agencies (ETH Board, ETH Zurich, PSI, SNF, UniZH, Canton Zurich, and SER); the Ministry of Science and Technology, Taipei; the Thailand Center of Excellence in Physics, the Institute for the Promotion of Teaching Science and Technology of Thailand, Special Task Force for Activating Research and the National Science and Technology Development Agency of Thailand; the Scientific and Technical Research Council of Turkey, and Turkish Atomic Energy Authority; the National Academy of Sciences of Ukraine, and State Fund for Fundamental Researches, Ukraine; the Science and Technology Facilities Council, U.K.; the US Department of Energy, and the US National Science Foundation.

Individuals have received support from the Marie-Curie programme and the European Research Council and EPLANET (European Union); the Leventis Foundation; the A. P. Sloan Foundation; the Alexander von Humboldt Foundation; the Belgian Federal Science Policy Office; the Fonds pour la Formation à la Recherche dans l'Industrie et dans l'Agriculture (FRIA-Belgium); the Agentschap voor Innovatie door Wetenschap en Technologie (IWT-Belgium); the Ministry of Education, Youth and Sports (MEYS) of the Czech Republic; the Council of Science and Industrial Research, India; the HOMING PLUS programme of the Foundation for Polish Science, cofinanced from European Union, Regional Development Fund, the Mobility Plus programme of the Ministry of Science and Higher Education, the National Science Center (Poland), contracts Harmonia 2014/14/M/ST2/00428, Opus 2014/13/B/ST2/02543, 2014/15/B/ST2/03998, and 2015/19/B/ST2/02861, Sonata-bis 2012/07/E/ST2/01406; the Thalis and Aristeia programmes cofinanced by EU-ESF and the Greek NSRF; the National Priorities Research Program by Qatar National Research Fund; the Programa Clarín-COFUND del Principado de Asturias; the Rachadapisek Sompot Fund for Postdoctoral Fellowship, Chulalongkorn University and the Chulalongkorn Academic into Its 2nd Century Project Advancement Project (Thailand); and the Welch Foundation, contract C-1845.

2017 JINST 12 P04023

References

[1] CMS collaboration, *Description and performance of track and primary-vertex reconstruction with the CMS tracker*, 2014 *JINST* **9** P10009 [arXiv:1405.6569].

[2] CMS collaboration, *The CMS Experiment at the CERN LHC*, 2008 *JINST* **3** S08004.

[3] CMS collaboration, *The CMS tracker: addendum to the Technical Design Report*, CERN-LHCC-2000-016 (2000).

[4] CMS collaboration, *Alignment of the CMS Silicon Tracker during Commissioning with Cosmic Rays*, 2010 *JINST* **5** T03009 [arXiv:0910.2505].

[5] CMS collaboration, *Alignment of the CMS Silicon Strip Tracker during stand-alone Commissioning*, 2009 *JINST* **4** T07001 [arXiv:0904.1220].

[6] CMS collaboration, *Alignment of the CMS tracker with LHC and cosmic ray data*, 2014 *JINST* **9** P06009 [arXiv:1403.2286].

[7] V. Blobel, C. Kleinwort and F. Meier, *Fast alignment of a complex tracking detector using advanced track models*, *Comput. Phys. Commun.* **182** (2011) 1760 [arXiv:1103.3909].

[8] V. Blobel, *Software alignment for tracking detectors*, *Nucl. Instrum. Meth.* **A 566** (2006) 5.

[9] B. Wittmer, R. Adolphi, M. Henke, A. Ostaptchouk, M. Thomas and S. Schael, *The laser alignment system for the CMS silicon microstrip tracker*, *Nucl. Instrum. Meth.* **A 581** (2007) 351.

[10] G. Sguazzoni et al., *Monitoring the stability of the ALEPH vertex detector*, *Nucl. Phys. Proc. Suppl.* **78** (1999) 301 [physics/9903031].

[11] K. Korcsak et al., *The Optical alignment system of the ZEUS microvertex detector*, *Nucl. Instrum. Meth.* **A 580** (2007) 1227 [arXiv:0808.0836].

[12] W. Wallraff, *The AMS-02 tracker alignment system for* 3*D position control with artificial laser generated straight tracks*, *Nucl. Instrum. Meth.* **A 572** (2007) 325.

[13] CMS collaboration, *Aligning the CMS Muon Chambers with the Muon Alignment System during an Extended Cosmic Ray Run*, 2010 *JINST* **5** T03019 [arXiv:0911.4770].

[14] D. Goldstein and D. Saltzberg, *The RASNIK real time relative alignment monitor for the CDF inner tracking detectors*, *Nucl. Instrum. Meth.* **A 506** (2003) 92 [hep-ex/0212025].

[15] S. Aefsky et al., *The optical alignment system of the ATLAS muon spectrometer endcaps*, 2008 *JINST* **3** P11005.

[16] P.A. Coe, D.F. Howell and R.B. Nickerson, *Frequency scanning interferometry in ATLAS: Remote, multiple, simultaneous and precise distance measurements in a hostile environment*, *Measur. Sci. Tech.* **15** (2004) 2175.

2017 JINST 12 P04023

The CMS collaboration

Yerevan Physics Institute, Yerevan, Armenia

A.M. Sirunyan, A. Tumasyan

Institut für Hochenergiephysik, Wien, Austria

W. Adam, E. Asilar, T. Bergauer, J. Brandstetter, E. Brondolin, M. Dragicevic, J. Erö, M. Flechl, M. Friedl, R. Frühwirth[1], V.M. Ghete, M. Hoch, C. Hartl, N. Hörmann, J. Hrubec, M. Jeitler[1], A. König, I. Krätschmer, D. Liko, T. Matsushita, I. Mikulec, D. Rabady, N. Rad, B. Rahbaran, H. Rohringer, J. Schieck[1], J. Strauss, W. Waltenberger, C.-E. Wulz[1]

Institute for Nuclear Problems, Minsk, Belarus

O. Dvornikov, V. Makarenko, V. Mossolov, J. Suarez Gonzalez, V. Zykunov

National Centre for Particle and High Energy Physics, Minsk, Belarus

N. Shumeiko

Universiteit Antwerpen, Antwerpen, Belgium

S. Alderweireldt, E.A. De Wolf, X. Janssen, J. Lauwers, M. Van De Klundert, H. Van Haevermaet, P. Van Mechelen, N. Van Remortel, A. Van Spilbeeck

Vrije Universiteit Brussel, Brussel, Belgium

S. Abu Zeid, F. Blekman, J. D'Hondt, N. Daci, I. De Bruyn, K. Deroover, S. Lowette, S. Moortgat, L. Moreels, A. Olbrechts, Q. Python, K. Skovpen, S. Tavernier, W. Van Doninck, P. Van Mulders, I. Van Parijs

Université Libre de Bruxelles, Bruxelles, Belgium

H. Brun, B. Clerbaux, G. De Lentdecker, H. Delannoy, G. Fasanella, L. Favart, R. Goldouzian, A. Grebenyuk, G. Karapostoli, T. Lenzi, A. Léonard, J. Luetic, T. Maerschalk, A. Marinov, A. Randle-conde, T. Seva, C. Vander Velde, P. Vanlaer, D. Vannerom, R. Yonamine, F. Zenoni, F. Zhang[2]

Ghent University, Ghent, Belgium

A. Cimmino, T. Cornelis, D. Dobur, A. Fagot, M. Gul, I. Khvastunov, D. Poyraz, S. Salva, R. Schöfbeck, M. Tytgat, W. Van Driessche, E. Yazgan, N. Zaganidis

Université Catholique de Louvain, Louvain-la-Neuve, Belgium

H. Bakhshiansohi, C. Beluffi[3], O. Bondu, S. Brochet, G. Bruno, A. Caudron, S. De Visscher, C. Delaere, M. Delcourt, B. Francois, A. Giammanco, A. Jafari, M. Komm, G. Krintiras, V. Lemaitre, A. Magitteri, A. Mertens, M. Musich, K. Piotrzkowski, L. Quertenmont, M. Selvaggi, M. Vidal Marono, S. Wertz

Université de Mons, Mons, Belgium

N. Beliy

Centro Brasileiro de Pesquisas Fisicas, Rio de Janeiro, Brazil

W.L. Aldá Júnior, F.L. Alves, G.A. Alves, L. Brito, C. Hensel, A. Moraes, M.E. Pol, P. Rebello Teles

2017 JINST 12 P04023

Universidade do Estado do Rio de Janeiro, Rio de Janeiro, Brazil

E. Belchior Batista Das Chagas, W. Carvalho, J. Chinellato[4], A. Custódio, E.M. Da Costa, G.G. Da Silveira[5], D. De Jesus Damiao, C. De Oliveira Martins, S. Fonseca De Souza, L.M. Huertas Guativa, H. Malbouisson, D. Matos Figueiredo, C. Mora Herrera, L. Mundim, H. Nogima, W.L. Prado Da Silva, A. Santoro, A. Sznajder, E.J. Tonelli Manganote[4], F. Torres Da Silva De Araujo, A. Vilela Pereira

Universidade Estadual Paulista [a], Universidade Federal do ABC [b], São Paulo, Brazil

S. Ahuja[a], C.A. Bernardes[a], S. Dogra[a], T.R. Fernandez Perez Tomei[a], E.M. Gregores[b], P.G. Mercadante[b], C.S. Moon[a], S.F. Novaes[a], Sandra S. Padula[a], D. Romero Abad[b], J.C. Ruiz Vargas[a]

Institute for Nuclear Research and Nuclear Energy, Sofia, Bulgaria

A. Aleksandrov, R. Hadjiiska, P. Iaydjiev, M. Rodozov, S. Stoykova, G. Sultanov, M. Vutova

University of Sofia, Sofia, Bulgaria

A. Dimitrov, I. Glushkov, L. Litov, B. Pavlov, P. Petkov

Beihang University, Beijing, China

W. Fang[6]

Institute of High Energy Physics, Beijing, China

M. Ahmad, J.G. Bian, G.M. Chen, H.S. Chen, M. Chen, Y. Chen[7], T. Cheng, C.H. Jiang, D. Leggat, Z. Liu, F. Romeo, M. Ruan, S.M. Shaheen, A. Spiezia, J. Tao, C. Wang, Z. Wang, H. Zhang, J. Zhao

State Key Laboratory of Nuclear Physics and Technology, Peking University, Beijing, China

Y. Ban, G. Chen, Q. Li, S. Liu, Y. Mao, S.J. Qian, D. Wang, Z. Xu

Universidad de Los Andes, Bogota, Colombia

C. Avila, A. Cabrera, L.F. Chaparro Sierra, C. Florez, J.P. Gomez, C.F. González Hernández, J.D. Ruiz Alvarez, J.C. Sanabria

University of Split, Faculty of Electrical Engineering, Mechanical Engineering and Naval Architecture, Split, Croatia

N. Godinovic, D. Lelas, I. Puljak, P.M. Ribeiro Cipriano, T. Sculac

University of Split, Faculty of Science, Split, Croatia

Z. Antunovic, M. Kovac

Institute Rudjer Boskovic, Zagreb, Croatia

V. Brigljevic, D. Ferencek, K. Kadija, B. Mesic, T. Susa

University of Cyprus, Nicosia, Cyprus

A. Attikis, G. Mavromanolakis, J. Mousa, C. Nicolaou, F. Ptochos, P.A. Razis, H. Rykaczewski, D. Tsiakkouri

Charles University, Prague, Czech Republic

M. Finger[8], M. Finger Jr.[8]

2017 JINST 12 P04023

Universidad San Francisco de Quito, Quito, Ecuador
E. Carrera Jarrin

Academy of Scientific Research and Technology of the Arab Republic of Egypt, Egyptian Network of High Energy Physics, Cairo, Egypt
A. Ellithi Kamel[9], M.A. Mahmoud[10,11], A. Radi[11,12]

National Institute of Chemical Physics and Biophysics, Tallinn, Estonia
M. Kadastik, L. Perrini, M. Raidal, A. Tiko, C. Veelken

Department of Physics, University of Helsinki, Helsinki, Finland
P. Eerola, J. Pekkanen, M. Voutilainen

Helsinki Institute of Physics, Helsinki, Finland
J. Härkönen, T. Järvinen, V. Karimäki, R. Kinnunen, T. Lampén, K. Lassila-Perini, S. Lehti, T. Lindén, P. Luukka, J. Tuominiemi, E. Tuovinen, L. Wendland

Lappeenranta University of Technology, Lappeenranta, Finland
J. Talvitie, T. Tuuva

IRFU, CEA, Université Paris-Saclay, Gif-sur-Yvette, France
M. Besancon, F. Couderc, M. Dejardin, D. Denegri, B. Fabbro, J.L. Faure, C. Favaro, F. Ferri, S. Ganjour, S. Ghosh, A. Givernaud, P. Gras, G. Hamel de Monchenault, P. Jarry, I. Kucher, E. Locci, M. Machet, J. Malcles, J. Rander, A. Rosowsky, M. Titov

Laboratoire Leprince-Ringuet, Ecole Polytechnique, IN2P3-CNRS, Palaiseau, France
A. Abdulsalam, I. Antropov, S. Baffioni, F. Beaudette, P. Busson, L. Cadamuro, E. Chapon, C. Charlot, O. Davignon, R. Granier de Cassagnac, M. Jo, S. Lisniak, P. Miné, M. Nguyen, C. Ochando, G. Ortona, P. Paganini, P. Pigard, S. Regnard, R. Salerno, Y. Sirois, T. Strebler, Y. Yilmaz, A. Zabi, A. Zghiche

Institut Pluridisciplinaire Hubert Curien (IPHC), Université de Strasbourg, CNRS-IN2P3
J.-L. Agram[13], J. Andrea, A. Aubin, D. Bloch, J.-M. Brom, M. Buttignol, E.C. Chabert, N. Chanon, C. Collard, E. Conte[13], X. Coubez, J.-C. Fontaine[13], D. Gelé, U. Goerlach, J. Hosselet, A.-C. Le Bihan, D. Tromson, P. Van Hove

Centre de Calcul de l'Institut National de Physique Nucleaire et de Physique des Particules, CNRS/IN2P3, Villeurbanne, France
S. Gadrat

Université de Lyon, Université Claude Bernard Lyon 1, CNRS-IN2P3, Institut de Physique Nucléaire de Lyon, Villeurbanne, France
S. Beauceron, C. Bernet, G. Boudoul, C.A. Carrillo Montoya, R. Chierici, C. Combaret, D. Contardo, B. Courbon, P. Depasse, H. El Mamouni, J. Fay, G. Galbit, S. Gascon, M. Gouzevitch, G. Grenier, B. Ille, F. Lagarde, I.B. Laktineh, M. Lethuillier, L. Mirabito, A.L. Pequegnot, S. Perries, A. Popov[14], D. Sabes, V. Sordini, M. Vander Donckt, P. Verdier, S. Viret, Y. Zoccarato

Georgian Technical University, Tbilisi, Georgia
T. Toriashvili[15]

2017 JINST 12 P04023

Tbilisi State University, Tbilisi, Georgia

D. Lomidze

RWTH Aachen University, I. Physikalisches Institut, Aachen, Germany

R. Adolphi, C. Autermann, S. Beranek, L. Feld, M.K. Kiesel, K. Klein, M. Lipinski, A. Ostapchuk, M. Preuten, M. Rauch, F. Raupach, S. Schael, C. Schomakers, J. Schulz, A. Schultz von Dratzig, T. Verlage, B. Wittmer, M. Wlochal, V. Zhukov[14]

RWTH Aachen University, III. Physikalisches Institut A, Aachen, Germany

A. Albert, M. Brodski, E. Dietz-Laursonn, D. Duchardt, M. Endres, M. Erdmann, S. Erdweg, T. Esch, R. Fischer, A. Güth, M. Hamer, T. Hebbeker, C. Heidemann, K. Hoepfner, S. Knutzen, M. Merschmeyer, A. Meyer, P. Millet, S. Mukherjee, M. Olschewski, K. Padeken, T. Pook, M. Radziej, H. Reithler, M. Rieger, F. Scheuch, L. Sonnenschein, D. Teyssier, S. Thüer

RWTH Aachen University, III. Physikalisches Institut B, Aachen, Germany

V. Cherepanov, G. Flügge, B. Kargoll, T. Kress, A. Künsken, J. Lingemann, T. Müller, A. Nehrkorn, A. Nowack, C. Pistone, O. Pooth, A. Stahl[16]

Deutsches Elektronen-Synchrotron, Hamburg, Germany

M. Aldaya Martin, T. Arndt, C. Asawatangtrakuldee, K. Beernaert, O. Behnke, U. Behrens, A.A. Bin Anuar, K. Borras[17], A. Campbell, P. Connor, C. Contreras-Campana, F. Costanza, C. Diez Pardos, G. Dolinska, G. Eckerlin, D. Eckstein, T. Eichhorn, E. Eren, E. Gallo[18], J. Garay Garcia, A. Geiser, A. Gizhko, J.M. Grados Luyando, A. Grohsjean, P. Gunnellini, A. Harb, J. Hauk, M. Hempel[19], H. Jung, A. Kalogeropoulos, O. Karacheban[19], M. Kasemann, J. Keaveney, C. Kleinwort, I. Korol, D. Krücker, W. Lange, A. Lelek, T. Lenz, J. Leonard, K. Lipka, A. Lobanov, W. Lohmann[19], R. Mankel, I.-A. Melzer-Pellmann, A.B. Meyer, G. Mittag, J. Mnich, A. Mussgiller, E. Ntomari, J. Olzem, D. Pitzl, R. Placakyte, A. Raspereza, B. Roland, M.Ö. Sahin, P. Saxena, T. Schoerner-Sadenius, S. Spannagel, N. Stefaniuk, G.P. Van Onsem, R. Walsh, C. Wissing

University of Hamburg, Hamburg, Germany

H. Biskop, V. Blobel, M. Centis Vignali, A.R. Draeger, T. Dreyer, E. Garutti, D. Gonzalez, J. Haller, M. Hoffmann, A. Junkes, R. Klanner, R. Kogler, N. Kovalchuk, T. Lapsien, I. Marchesini, D. Marconi, M. Matysek, M. Meyer, M. Niedziela, D. Nowatschin, F. Pantaleo[16], T. Peiffer, A. Perieanu, J. Poehlsen, C. Scharf, P. Schleper, A. Schmidt, S. Schumann, J. Schwandt, H. Stadie, G. Steinbrück, F.M. Stober, M. Stöver, H. Tholen, D. Troendle, E. Usai, L. Vanelderen, A. Vanhoefer, B. Vormwald, J. Wellhausen

Institut für Experimentelle Kernphysik, Karlsruhe, Germany

M. Abbas, M. Akbiyik, C. Amstutz, C. Barth, S. Baur, C. Baus, J. Berger, E. Butz, M. Casele, R. Caspart, T. Chwalek, F. Colombo, W. De Boer, A. Dierlamm, S. Fink, B. Freund, R. Friese, M. Giffels, A. Gilbert, P. Goldenzweig, D. Haitz, F. Hartmann[16], S.M. Heindl, U. Husemann, I. Katkov, A. Kornmeyer,[14], S. Kudella, H. Mildner, M.U. Mozer, Th. Müller, M. Plagge, G. Quast, K. Rabbertz, S. Röcker, F. Roscher, M. Schröder, I. Shvetsov, G. Sieber, H.J. Simonis, R. Ulrich, S. Wayand, M. Weber, T. Weiler, S. Williamson, C. Wöhrmann, R. Wolf

2017 JINST 12 P04023

Institute of Nuclear and Particle Physics (INPP), NCSR Demokritos, Aghia Paraskevi, Greece
G. Anagnostou, G. Daskalakis, T. Geralis, V.A. Giakoumopoulou, A. Kyriakis, D. Loukas, I. Topsis-Giotis

National and Kapodistrian University of Athens, Athens, Greece
S. Kesisoglou, A. Panagiotou, N. Saoulidou, E. Tziaferi

University of Ioánnina, Ioánnina, Greece
I. Evangelou, G. Flouris, C. Foudas, P. Kokkas, N. Loukas, N. Manthos, I. Papadopoulos, E. Paradas

MTA-ELTE Lendület CMS Particle and Nuclear Physics Group, Eötvös Loránd University, Budapest, Hungary
N. Filipovic, G. Pasztor

Wigner Research Centre for Physics, Budapest, Hungary
G. Bencze, C. Hajdu, D. Horvath[20], F. Sikler, V. Veszpremi, G. Vesztergombi[21], A.J. Zsigmond

Institute of Nuclear Research ATOMKI, Debrecen, Hungary
N. Beni, S. Czellar, J. Karancsi[22], A. Makovec, J. Molnar, Z. Szillasi

Institute of Physics, University of Debrecen
M. Bartók[21], P. Raics, Z.L. Trocsanyi, B. Ujvari

Indian Institute of Science (IISc)
J.R. Komaragiri

National Institute of Science Education and Research, Bhubaneswar, India
S. Bahinipati[23], S. Bhowmik[24], S. Choudhury[25], P. Mal, K. Mandal, A. Nayak[26], D.K. Sahoo[23], N. Sahoo, S.K. Swain

Panjab University, Chandigarh, India
S. Bansal, S.B. Beri, V. Bhatnagar, R. Chawla, U.Bhawandeep, A.K. Kalsi, A. Kaur, M. Kaur, R. Kumar, P. Kumari, A. Mehta, M. Mittal, J.B. Singh, G. Walia

University of Delhi, Delhi, India
Ashok Kumar, A. Bhardwaj, B.C. Choudhary, R.B. Garg, S. Keshri, S. Malhotra, M. Naimuddin, K. Ranjan, R. Sharma, V. Sharma

Saha Institute of Nuclear Physics, Kolkata, India
R. Bhattacharya, S. Bhattacharya, K. Chatterjee, S. Dey, S. Dutt, S. Dutta, S. Ghosh, N. Majumdar, A. Modak, K. Mondal, S. Mukhopadhyay, S. Nandan, A. Purohit, A. Roy, D. Roy, S. Roy Chowdhury, S. Sarkar, M. Sharan, S. Thakur

Indian Institute of Technology Madras, Madras, India
P.K. Behera

Bhabha Atomic Research Centre, Mumbai, India
R. Chudasama, D. Dutta, V. Jha, V. Kumar, A.K. Mohanty[16], P.K. Netrakanti, L.M. Pant, P. Shukla, A. Topkar

2017 JINST 12 P04023

Tata Institute of Fundamental Research-A, Mumbai, India

T. Aziz, S. Dugad, G. Kole, B. Mahakud, S. Mitra, G.B. Mohanty, B. Parida, N. Sur, B. Sutar

Tata Institute of Fundamental Research-B, Mumbai, India

S. Banerjee, R.K. Dewanjee, S. Ganguly, M. Guchait, Sa. Jain, S. Kumar, M. Maity[24], G. Majumder, K. Mazumdar, T. Sarkar[24], N. Wickramage[27]

Indian Institute of Science Education and Research (IISER), Pune, India

S. Chauhan, S. Dube, V. Hegde, A. Kapoor, K. Kothekar, S. Pandey, A. Rane, S. Sharma

Institute for Research in Fundamental Sciences (IPM), Tehran, Iran

H. Bakhshiansohl, S. Chenarani[28], E. Eskandari Tadavani, S.M. Etesami[28], M. Khakzad, M. Mohammadi Najafabadi, M. Naseri, S. Paktinat Mehdiabadi[29], F. Rezaei Hosseinabadi, B. Safarzadeh[30], M. Zeinali

University College Dublin, Dublin, Ireland

M. Felcini, M. Grunewald

INFN Sezione di Bari [a], Università di Bari [b], Politecnico di Bari [c], Bari, Italy

M. Abbrescia[a,b], C. Calabria[a,b], C. Caputo[a,b], P. Cariola[a], A. Colaleo[a], D. Creanza[a,c], L. Cristella[a,b], N. De Filippis[a,c], M. De Palma[a,b], L. Fiore[a], G. Iaselli[a,c], G. Maggi[a,c], M. Maggi[a], G. Miniello[a,b], S. My[a,b], S. Nuzzo[a,b], A. Pompili[a,b], G. Pugliese[a,c], R. Radogna[a,b], A. Ranieri[a], G. Selvaggi[a,b], A. Sharma[a], L. Silvestris[a,16], R. Venditti[a,b], P. Verwilligen[a]

INFN Sezione di Bologna [a], Università di Bologna [b], Bologna, Italy

G. Abbiendi[a], C. Battilana, D. Bonacorsi[a,b], S. Braibant-Giacomelli[a,b], L. Brigliadori[a,b], R. Campanini[a,b], P. Capiluppi[a,b], A. Castro[a,b], F.R. Cavallo[a], S.S. Chhibra[a,b], G. Codispoti[a,b], M. Cuffiani[a,b], G.M. Dallavalle[a], F. Fabbri[a], A. Fanfani[a,b], D. Fasanella[a,b], P. Giacomelli[a], C. Grandi[a], L. Guiducci[a,b], S. Marcellini[a], G. Masetti[a], A. Montanari[a], F.L. Navarria[a,b], A. Perrotta[a], A.M. Rossi[a,b], T. Rovelli[a,b], G.P. Siroli[a,b], N. Tosi[a,b,16]

INFN Sezione di Catania [a], Università di Catania [b], Catania, Italy

S. Albergo[a,b], S. Costa[a,b], A. Di Mattia[a], F. Giordano[a,b], R. Potenza[a,b], A. Tricomi[a,b], C. Tuve[a,b]

INFN Sezione di Firenze [a], Università di Firenze [b], Firenze, Italy

G. Barbagli[a], V. Ciulli[a,b], C. Civinini[a], R. D'Alessandro[a,b], E. Focardi[a,b], G. Latino[a,b], P. Lenzi[a,b], M. Meschini[a], S. Paoletti[a], L. Russo[a,31], G. Sguazzoni[a], D. Strom[a], L. Viliani[a,b,16]

INFN Laboratori Nazionali di Frascati, Frascati, Italy

L. Benussi, S. Bianco, F. Fabbri, D. Piccolo, F. Primavera[16]

INFN Sezione di Genova [a], Università di Genova [b], Genova, Italy

V. Calvelli[a,b], F. Ferro[a], M.R. Monge[a,b], E. Robutti[a], S. Tosi[a,b]

INFN Sezione di Milano-Bicocca [a], Università di Milano-Bicocca [b], Milano, Italy

L. Brianza[a,b,16], F. Brivio[a,b], V. Ciriolo, M.E. Dinardo[a,b], S. Fiorendi[a,b,16], S. Gennai[a], A. Ghezzi[a,b], P. Govoni[a,b], M. Malberti[a,b], S. Malvezzi[a], R.A. Manzoni[a,b], D. Menasce[a], L. Moroni[a], M. Paganoni[a,b], D. Pedrini[a], S. Pigazzini[a,b], S. Ragazzi[a,b], T. Tabarelli de Fatis[a,b]

2017 JINST 12 P04023

INFN Sezione di Napoli [a], Università di Napoli 'Federico II' [b], Napoli, Italy, Università della Basilicata [c], Potenza, Italy, Università G. Marconi [d], Roma, Italy

S. Buontempo[a], N. Cavallo[a,c], G. De Nardo, S. Di Guida[a,d,16], M. Esposito[a,b], F. Fabozzi[a,c], F. Fienga[a,b], A.O.M. Iorio[a,b], G. Lanza[a], L. Lista[a], S. Meola[a,d,16], P. Paolucci[a,16], C. Sciacca[a,b], F. Thyssen[a]

INFN Sezione di Padova [a], Università di Padova [b], Padova, Italy, Università di Trento [c], Trento, Italy

P. Azzi[a,16], N. Bacchetta[a], L. Benato[a,b], D. Bisello[a,b], A. Boletti[a,b], R. Carlin[a,b], P. Checchia[a], M. Dall'Osso[a,b], P. De Castro Manzano[a], T. Dorigo[a], U. Dosselli[a], F. Gasparini[a,b], S. Lacaprara[a], M. Margoni[a,b], G. Maron[a,32], A.T. Meneguzzo[a,b], M. Michelotto[a], F. Montecassiano[a], J. Pazzini[a,b], N. Pozzobon[a,b], P. Ronchese[a,b], F. Simonetto[a,b], E. Torassa[a], M. Zanetti[a,b], P. Zotto[a,b], G. Zumerle[a,b]

INFN Sezione di Pavia [a], Università di Pavia [b], Pavia, Italy

A. Braghieri[a], D. Comotti[a,b], F. De Canio[a], F. Fallavollita[a,b], A. Magnani[a,b], P. Montagna[a,b], B. Nodari[a], S.P. Ratti[a,b], V. Re[a], C. Riccardi[a,b], E. Riceputi[a], P. Salvini[a], I. Vai[a,b], P. Vitulo[a,b]

INFN Sezione di Perugia [a], Università di Perugia [b], Perugia, Italy

L. Alunni Solestizi[a,b], G.M. Bilei[a], D. Ciangottini[a,b], L. Fanò[a,b], P. Lariccia[a,b], R. Leonardi[a,b], G. Mantovani[a,b], V. Mariani[a,b], M. Menichelli[a], A. Saha[a], A. Santocchia[a,b], L. Storchi[a]

INFN Sezione di Pisa [a], Università di Pisa [b], Scuola Normale Superiore di Pisa [c], Pisa, Italy

K. Androsov[a,31], P. Azzurri[a,16], G. Bagliesi[a], J. Bernardini[a], T. Boccali[a], R. Castaldi[a], M.A. Ciocci[a,31], R. Dell'Orso[a], S. Donato[a,c], G. Fedi, A. Giassi[a], M.T. Grippo[a,31], F. Ligabue[a,c], T. Lomtadze[a], L. Martini[a,b], A. Messineo[a,b], F. Morsani[a], F. Palla[a], A. Rizzi[a,b], A. Savoy-Navarro[a,33], P. Spagnolo[a], R. Tenchini[a], G. Tonelli[a,b], A. Venturi[a], P.G. Verdini[a]

INFN Sezione di Roma [a], Università di Roma [b], Roma, Italy

L. Barone[a,b], F. Cavallari[a], M. Cipriani[a,b], D. Del Re[a,b,16], M. Diemoz[a], S. Gelli[a,b], E. Longo[a,b], F. Margaroli[a,b], B. Marzocchi[a,b], P. Meridiani[a], G. Organtini[a,b], R. Paramatti[a], F. Preiato[a,b], S. Rahatlou[a,b], C. Rovelli[a], F. Santanastasio[a,b]

INFN Sezione di Torino [a], Università di Torino [b], Torino, Italy, Università del Piemonte Orientale [c], Novara, Italy

N. Amapane[a,b], R. Arcidiacono[a,c,16], S. Argiro[a,b], M. Arneodo[a,c], N. Bartosik[a], R. Bellan[a,b], C. Biino[a], N. Cartiglia[a], F. Cenna[a,b], M. Costa[a,b], R. Covarelli[a,b], A. Degano[a,b], N. Demaria[a], L. Finco[a,b], B. Kiani[a,b], C. Mariotti[a], S. Maselli[a], E. Migliore[a,b], V. Monaco[a,b], E. Monteil[a,b], M. Monteno[a], M.M. Obertino[a,b], L. Pacher[a,b], N. Pastrone[a], M. Pelliccioni[a], G.L. Pinna Angioni[a,b], F. Ravera[a,b], A. Rivetti[a], A. Romero[a,b], M. Ruspa[a,c], R. Sacchi[a,b], K. Shchelina[a,b], V. Sola[a], A. Solano[a,b], A. Staiano[a], P. Traczyk[a,b]

INFN Sezione di Trieste [a], Università di Trieste [b], Trieste, Italy

S. Belforte[a], M. Casarsa[a], F. Cossutti[a], G. Della Ricca[a,b], A. Zanetti[a]

Kyungpook National University, Daegu, Korea

D.H. Kim, G.N. Kim, M.S. Kim, S. Lee, S.W. Lee, Y.D. Oh, S. Sekmen, D.C. Son, Y.C. Yang

2017 JINST 12 P04023

Chonbuk National University, Jeonju, Korea
A. Lee

Chonnam National University, Institute for Universe and Elementary Particles, Kwangju, Korea
H. Kim

Hanyang University, Seoul, Korea
J.A. Brochero Cifuentes, T.J. Kim

Korea University, Seoul, Korea
S. Cho, S. Choi, Y. Go, D. Gyun, S. Ha, B. Hong, Y. Jo, Y. Kim, K. Lee, K.S. Lee, S. Lee, J. Lim, S.K. Park, Y. Roh

Seoul National University, Seoul, Korea
J. Almond, J. Kim, H. Lee, S.B. Oh, B.C. Radburn-Smith, S.h. Seo, U.K. Yang, H.D. Yoo, G.B. Yu

University of Seoul, Seoul, Korea
M. Choi, H. Kim, J.H. Kim, J.S.H. Lee, I.C. Park, G. Ryu, M.S. Ryu

Sungkyunkwan University, Suwon, Korea
Y. Choi, J. Goh, C. Hwang, J. Lee, I. Yu

Vilnius University, Vilnius, Lithuania
V. Dudenas, A. Juodagalvis, J. Vaitkus

National Centre for Particle Physics, Universiti Malaya, Kuala Lumpur, Malaysia
I. Ahmed, Z.A. Ibrahim, M.A.B. Md Ali[34], F. Mohamad Idris[35], W.A.T. Wan Abdullah, M.N. Yusli, Z. Zolkapli

Centro de Investigacion y de Estudios Avanzados del IPN, Mexico City, Mexico
H. Castilla-Valdez, E. De La Cruz-Burelo, I. Heredia-De La Cruz[36], A. Hernandez-Almada, R. Lopez-Fernandez, R. Magaña Villalba, J. Mejia Guisao, A. Sanchez-Hernandez

Universidad Iberoamericana, Mexico City, Mexico
S. Carrillo Moreno, C. Oropeza Barrera, F. Vazquez Valencia

Benemerita Universidad Autonoma de Puebla, Puebla, Mexico
S. Carpinteyro, I. Pedraza, H.A. Salazar Ibarguen, C. Uribe Estrada

Universidad Autónoma de San Luis Potosí, San Luis Potosí, Mexico
A. Morelos Pineda

University of Auckland, Auckland, New Zealand
D. Krofcheck

University of Canterbury, Christchurch, New Zealand
P.H. Butler

National Centre for Physics, Quaid-I-Azam University, Islamabad, Pakistan
A. Ahmad, M. Ahmad, Q. Hassan, H.R. Hoorani, W.A. Khan, A. Saddique, M.A. Shah, M. Shoaib, M. Waqas

2017 JINST 12 P04023

National Centre for Nuclear Research, Swierk, Poland

H. Bialkowska, M. Bluj, B. Boimska, T. Frueboes, M. Górski, M. Kazana, K. Nawrocki, K. Romanowska-Rybinska, M. Szleper, P. Zalewski

Institute of Experimental Physics, Faculty of Physics, University of Warsaw, Warsaw, Poland

K. Bunkowski, A. Byszuk[37], K. Doroba, A. Kalinowski, M. Konecki, J. Krolikowski, M. Misiura, M. Olszewski, M. Walczak

Laboratório de Instrumentação e Física Experimental de Partículas, Lisboa, Portugal

P. Bargassa, C. Beirão Da Cruz E Silva, B. Calpas, A. Di Francesco, P. Faccioli, P.G. Ferreira Parracho, M. Gallinaro, J. Hollar, N. Leonardo, L. Lloret Iglesias, M.V. Nemallapudi, J. Rodrigues Antunes, J. Seixas, O. Toldaiev, D. Vadruccio, J. Varela, P. Vischia

Joint Institute for Nuclear Research, Dubna, Russia

S. Afanasiev, P. Bunin, M. Gavrilenko, I. Golutvin, I. Gorbunov, A. Kamenev, V. Karjavin, A. Lanev, A. Malakhov, V. Matveev[38,39], V. Palichik, V. Perelygin, S. Shmatov, S. Shulha, N. Skatchkov, V. Smirnov, N. Voytishin, A. Zarubin

Petersburg Nuclear Physics Institute, Gatchina (St. Petersburg), Russia

L. Chtchipounov, V. Golovtsov, Y. Ivanov, V. Kim[40], E. Kuznetsova[41], V. Murzin, V. Oreshkin, V. Sulimov, A. Vorobyev

Institute for Nuclear Research, Moscow, Russia

Yu. Andreev, A. Dermenev, S. Gninenko, N. Golubev, A. Karneyeu, M. Kirsanov, N. Krasnikov, A. Pashenkov, D. Tlisov, A. Toropin

Institute for Theoretical and Experimental Physics, Moscow, Russia

V. Epshteyn, V. Gavrilov, N. Lychkovskaya, V. Popov, I. Pozdnyakov, G. Safronov, A. Spiridonov, M. Toms, E. Vlasov, A. Zhokin

Moscow Institute of Physics and Technology, Moscow, Russia

A. Bylinkin[39]

P.N. Lebedev Physical Institute, Moscow, Russia

V. Andreev, M. Azarkin[39], I. Dremin[39], M. Kirakosyan, A. Leonidov[39], A. Terkulov

Skobeltsyn Institute of Nuclear Physics, Lomonosov Moscow State University, Moscow, Russia

A. Baskakov, A. Belyaev, E. Boos, M. Dubinin[42], L. Dudko, A. Ershov, A. Gribushin, A. Kaminskiy[43], V. Klyukhin, O. Kodolova, I. Lokhtin, I. Miagkov, S. Obraztsov, S. Petrushanko, V. Savrin

Novosibirsk State University (NSU), Novosibirsk, Russia

V. Blinov[44], Y.Skovpen[44], D. Shtol[44]

State Research Center of Russian Federation, Institute for High Energy Physics, Protvino, Russia

I. Azhgirey, I. Bayshev, S. Bitioukov, D. Elumakhov, V. Kachanov, A. Kalinin, D. Konstantinov, V. Krychkine, V. Petrov, R. Ryutin, A. Sobol, S. Troshin, N. Tyurin, A. Uzunian, A. Volkov

2017 JINST 12 P04023

University of Belgrade, Faculty of Physics and Vinca Institute of Nuclear Sciences, Belgrade, Serbia

P. Adzic[45], P. Cirkovic, D. Devetak, M. Dordevic, J. Milosevic, V. Rekovic

Centro de Investigaciones Energéticas Medioambientales y Tecnológicas (CIEMAT), Madrid, Spain

J. Alcaraz Maestre, M. Barrio Luna, E. Calvo, M. Cerrada, M. Chamizo Llatas, N. Colino, B. De La Cruz, A. Delgado Peris, A. Escalante Del Valle, C. Fernandez Bedoya, J.P. Fernández Ramos, J. Flix, M.C. Fouz, P. Garcia-Abia, O. Gonzalez Lopez, S. Goy Lopez, J.M. Hernandez, M.I. Josa, E. Navarro De Martino, A. Pérez-Calero Yzquierdo, J. Puerta Pelayo, A. Quintario Olmeda, I. Redondo, L. Romero, M.S. Soares

Universidad Autónoma de Madrid, Madrid, Spain

J.F. de Trocóniz, M. Missiroli, D. Moran

Universidad de Oviedo, Oviedo, Spain

J. Cuevas, J. Fernandez Menendez, I. Gonzalez Caballero, J.R. González Fernández, E. Palencia Cortezon, S. Sanchez Cruz, I. Suárez Andrés, J.M. Vizan Garcia

Instituto de Física de Cantabria (IFCA), CSIC-Universidad de Cantabria, Santander, Spain

I.J. Cabrillo, A. Calderon, E. Curras, M. Fernandez, J. Garcia-Ferrero, G. Gomez, A. Lopez Virto, J. Marco, C. Martinez Rivero, F. Matorras, J. Piedra Gomez, T. Rodrigo, A. Ruiz-Jimeno, L. Scodellaro, N. Trevisani, I. Vila, R. Vilar Cortabitarte

CERN, European Organization for Nuclear Research, Geneva, Switzerland

D. Abbaneo, E. Auffray, G. Auzinger, P. Baillon, A.H. Ball, D. Barney, G. Blanchot, P. Bloch, A. Bocci, J. Bonnaud, C. Botta, T. Camporesi, A. Caratelli, R. Castello, M. Cepeda, D. Ceresa, G. Cerminara, Y. Chen, K. Cichy, D. d'Enterria, A. Dabrowski, V. Daponte, A. David, M. De Gruttola, A. De Roeck, S. Detraz, E. Di Marco[46], M. Dobson, O. Dondelewski, B. Dorney, T. du Pree, D. Duggan, M. Dünser, N. Dupont, A. Elliott-Peisert, P. Everaerts, F. Faccio, S. Fartoukh, G. Franzoni, J. Fulcher, W. Funk, T. Gadek, D. Gigi, K. Gill, M. Girone, F. Glege, D. Gulhan, S. Gundacker, M. Guthoff, P. Harris, J. Hegeman, V. Innocente, P. Janot, L. M. Jara Casas, J. Kaplon, J. Kieseler, H. Kirschenmann, V. Knünz, A. Kornmayer[16], M.J. Kortelainen, K. Kousouris, M. Krammer[1], C. Lange, P. Lecoq, P. Lenoir, C. Lourenço, M.T. Lucchini, S. Marconi, L. Malgeri, M. Mannelli, A. Martelli, S. Martina, F. Meijers, J.A. Merlin, S. Mersi, E. Meschi, S. Michelis, P. Milenovic[47], F. Moortgat, S. Morovic, M. Mulders, H. Neugebauer, S. Orfanelli, L. Orsini, L. Pape, S. Pavis, E. Perez, M. Peruzzi, A. Petrilli, G. Petrucciani, A. Pfeiffer, M. Pierini, A. Racz, T. Reis, G. Rolandi[48], P. Rose, M. Rovere, H. Sakulin, J.B. Sauvan, C. Schäfer, C. Schwick, M. Seidel, A. Sharma, P. Silva, P. Sphicas[49], J. Steggemann, M. Stoye, Y. Takahashi, M. Tosi, D. Treille, A. Triossi, A. Tsirou, V. Veckalns[50], G.I. Veres[21], B. Verlaat, M. Verweij, N. Wardle, H.K. Wöhri, A. Zagozdzinska[37], W.D. Zeuner, L. Zwalinski

Paul Scherrer Institut, Villigen, Switzerland

W. Bertl, K. Deiters, W. Erdmann, R. Horisberger, Q. Ingram, H.C. Kaestli, D. Kotlinski, U. Langenegger, T. Rohe

2017 JINST 12 P04023

Institute for Particle Physics, ETH Zurich, Zurich, Switzerland

F. Bachmair, L. Bäni, P. Berger, L. Bianchini, B. Casal, G. Dissertori, M. Dittmar, M. Donegà, C. Grab, C. Heidegger, D. Hits, J. Hoss, G. Kasieczka, W. Lustermann, B. Mangano, M. Marionneau, P. Martinez Ruiz del Arbol, M. Masciovecchio, M.T. Meinhard, D. Meister, F. Micheli, P. Musella, F. Nessi-Tedaldi, F. Pandolfi, J. Pata, F. Pauss, G. Perrin, L. Perrozzi, M. Quittnat, M. Rossini, M. Schönenberger, A. Starodumov[51], V.R. Tavolaro, K. Theofilatos, R. Wallny, D. Zhu

Universität Zürich, Zurich, Switzerland

T.K. Aarrestad, C. Amsler[52], K. Bösiger, L. Caminada, M.F. Canelli, A. De Cosa, C. Galloni, A. Hinzmann, T. Hreus, B. Kilminster, R. Maier, J. Ngadiuba, D. Pinna, G. Rauco, P. Robmann, D. Salerno, C. Seitz, Y. Yang, A. Zucchetta

National Central University, Chung-Li, Taiwan

V. Candelise, T.H. Doan, Sh. Jain, R. Khurana, M. Konyushikhin, C.M. Kuo, W. Lin, A. Pozdnyakov, S.S. Yu

National Taiwan University (NTU), Taipei, Taiwan

Arun Kumar, P. Chang, Y.H. Chang, Y. Chao, K.F. Chen, P.H. Chen, F. Fiori, W.-S. Hou, Y. Hsiung, Y.F. Liu, R.-S. Lu, M. Miñano Moya, E. Paganis, A. Psallidas, J.f. Tsai

Chulalongkorn University, Faculty of Science, Department of Physics, Bangkok, Thailand

B. Asavapibhop, G. Singh, N. Srimanobhas, N. Suwonjandee

Cukurova University - Physics Department, Science and Art Faculty

A. Adiguzel, S. Cerci[53], S. Damarseckin, Z.S. Demiroglu, C. Dozen, I. Dumanoglu, S. Girgis, G. Gokbulut, Y. Guler, I. Hos[54], E.E. Kangal[55], O. Kara, A. Kayis Topaksu, U. Kiminsu, M. Oglakci, G. Onengut[56], K. Ozdemir[57], D. Sunar Cerci[53], B. Tali[53], S. Turkcapar, I.S. Zorbakir, C. Zorbilmez

Middle East Technical University, Physics Department, Ankara, Turkey

B. Bilin, S. Bilmis, B. Isildak[58], G. Karapinar[59], M. Yalvac, M. Zeyrek

Bogazici University, Istanbul, Turkey

E. Gülmez, M. Kaya[60], O. Kaya[61], E.A. Yetkin[62], T. Yetkin[63]

Istanbul Technical University, Istanbul, Turkey

A. Cakir, K. Cankocak, S. Sen[64]

Institute for Scintillation Materials of National Academy of Science of Ukraine, Kharkov, Ukraine

B. Grynyov

National Scientific Center, Kharkov Institute of Physics and Technology, Kharkov, Ukraine

L. Levchuk, P. Sorokin

University of Bristol, Bristol, United Kingdom

R. Aggleton, F. Ball, L. Beck, J.J. Brooke, D. Burns, E. Clement, D. Cussans, H. Flacher, J. Goldstein, M. Grimes, G.P. Heath, H.F. Heath, J. Jacob, L. Kreczko, C. Lucas, D.M. Newbold[65], S. Paramesvaran, A. Poll, T. Sakuma, S. Seif El Nasr-storey, D. Smith, V.J. Smith

2017 JINST 12 P04023

Rutherford Appleton Laboratory, Didcot, United Kingdom

K.W. Bell, A. Belyaev[66], C. Brew, R.M. Brown, L. Calligaris, D. Cieri, D.J.A. Cockerill, J.A. Coughlan, K. Harder, S. Harper, E. Olaiya, D. Petyt, C.H. Shepherd-Themistocleous, A. Thea, I.R. Tomalin, T. Williams

Imperial College, London, United Kingdom

M. Baber, R. Bainbridge, O. Buchmuller, A. Bundock, D. Burton, S. Casasso, M. Citron, D. Colling, L. Corpe, P. Dauncey, G. Davies, A. De Wit, M. Della Negra, R. Di Maria, P. Dunne, A. Elwood, D. Futyan, Y. Haddad, G. Hall, G. Iles, T. James, R. Lane, C. Laner, R. Lucas[65], L. Lyons, A.-M. Magnan, S. Malik, L. Mastrolorenzo, J. Nash, A. Nikitenko[51], J. Pela, B. Penning, M. Pesaresi, D.M. Raymond, A. Richards, A. Rose, E. Scott, C. Seez, S. Summers, A. Tapper, K. Uchida, M. Vazquez Acosta[67], T. Virdee[16], J. Wright, S.C. Zenz

Brunel University, Uxbridge, United Kingdom

J.E. Cole, P.R. Hobson, A. Khan, P. Kyberd, A. Morton, I.D. Reid, P. Symonds, L. Teodorescu, M. Turner

Baylor University, Waco, U.S.A.

A. Borzou, K. Call, J. Dittmann, K. Hatakeyama, H. Liu, N. Pastika

Catholic University of America

R. Bartek, A. Dominguez

The University of Alabama, Tuscaloosa, U.S.A.

A. Buccilli, S.I. Cooper, C. Henderson, P. Rumerio, C. West

Boston University, Boston, U.S.A.

D. Arcaro, A. Avetisyan, T. Bose, D. Gastler, D. Rankin, C. Richardson, J. Rohlf, L. Sulak, D. Zou

Brown University, Providence, U.S.A.

G. Benelli, D. Cutts, A. Garabedian, J. Hakala, U. Heintz, J.M. Hogan, O. Jesus, K.H.M. Kwok, E. Laird, G. Landsberg, Z. Mao, M. Narain, J. Nelson, S. Piperov, S. Sagir, E. Spencer, J. Swanson, R. Syarif, D. Tersegno, J. Watson-Daniels

University of California, Davis, Davis, U.S.A.

R. Breedon, D. Burns, M. Calderon De La Barca Sanchez, S. Chauhan, M. Chertok, J. Conway, R. Conway, P.T. Cox, R. Erbacher, C. Flores, G. Funk, M. Gardner, W. Ko, R. Lander, C. Mclean, M. Mulhearn, D. Pellett, J. Pilot, S. Shalhout, M. Shi, J. Smith, M. Squires, D. Stolp, K. Tos, M. Tripathi

University of California, Los Angeles, U.S.A.

M. Bachtis, C. Bravo, R. Cousins, A. Dasgupta, A. Florent, J. Hauser, M. Ignatenko, N. Mccoll, D. Saltzberg, C. Schnaible, V. Valuev, M. Weber

University of California, Riverside, Riverside, U.S.A.

E. Bouvier, K. Burt, R. Clare, J. Ellison, J.W. Gary, S.M.A. Ghiasi Shirazi, G. Hanson, J. Heilman, P. Jandir, E. Kennedy, F. Lacroix, O.R. Long, M. Olmedo Negrete, M.I. Paneva, A. Shrinivas, W. Si, H. Wei, S. Wimpenny, B. R. Yates

2017 JINST 12 P04023

University of California, San Diego, La Jolla, U.S.A.

J.G. Branson, G.B. Cerati, S. Cittolin, M. Derdzinski, R. Gerosa, A. Holzner, D. Klein, V. Krutelyov, J. Letts, I. Macneill, D. Olivito, S. Padhi, M. Pieri, M. Sani, V. Sharma, S. Simon, M. Tadel, A. Vartak, S. Wasserbaech[68], C. Welke, J. Wood, F. Würthwein, A. Yagil, G. Zevi Della Porta

University of California, Santa Barbara - Department of Physics, Santa Barbara, U.S.A.

N. Amin, R. Bhandari, J. Bradmiller-Feld, C. Campagnari, A. Dishaw, V. Dutta, M. Franco Sevilla, C. George, F. Golf, L. Gouskos, J. Gran, R. Heller, J. Incandela, S.D. Mullin, A. Ovcharova, H. Qu, J. Richman, D. Stuart, I. Suarez, J. Yoo

California Institute of Technology, Pasadena, U.S.A.

D. Anderson, J. Bendavid, A. Bornheim, J. Bunn, J. Duarte, J.M. Lawhorn, A. Mott, H.B. Newman, C. Pena, M. Spiropulu, J.R. Vlimant, S. Xie, R.Y. Zhu

Carnegie Mellon University, Pittsburgh, U.S.A.

M.B. Andrews, T. Ferguson, M. Paulini, J. Russ, M. Sun, H. Vogel, I. Vorobiev, M. Weinberg

University of Colorado Boulder, Boulder, U.S.A.

J.P. Cumalat, W.T. Ford, F. Jensen, A. Johnson, M. Krohn, S. Leontsinis, T. Mulholland, K. Stenson, S.R. Wagner

Cornell University, Ithaca, U.S.A.

J. Alexander, J. Chaves, J. Chu, S. Dittmer, K. Mcdermott, N. Mirman, G. Nicolas Kaufman, J.R. Patterson, A. Rinkevicius, A. Ryd, L. Skinnari, L. Soffi, S.M. Tan, Z. Tao, J. Thom, J. Tucker, P. Wittich, M. Zientek

Fairfield University, Fairfield, U.S.A.

D. Winn

Fermi National Accelerator Laboratory, Batavia, U.S.A.

S. Abdullin, M. Albrow, G. Apollinari, A. Apresyan, B. Baldin, S. Banerjee, L.A.T. Bauerdick, A. Beretvas, J. Berryhill, P.C. Bhat, G. Bolla, K. Burkett, J.N. Butler, A. Canepa, H.W.K. Cheung, F. Chlebana, J. Chramowicz, D. Christian, S. Cihangir[†], M. Cremonesi, V.D. Elvira, I. Fisk, J. Freeman, C. Gingu, E. Gottschalk, L. Gray, D. Green, S. Grünendahl, O. Gutsche, D. Hare, R.M. Harris, S. Hasegawa, J. Hirschauer, J. Hoff, M. Hrycyk, Z. Hu, B. Jayatilaka, S. Jindariani, M. Johnson, U. Joshi, F. Kahlid, B. Klima, B. Kreis, S. Lammel, J. Linacre, D. Lincoln, R. Lipton, M. Liu, T. Liu, R. Lopes De Sá, J. Lykken, K. Maeshima, N. Magini, J.M. Marraffino, S. Maruyama, D. Mason, M. Matulik, P. McBride, P. Merkel, S. Mrenna, S. Nahn, V. O'Dell, K. Pedro, O. Prokofyev, G. Rakness, L. Ristori, E. Sexton-Kennedy, A. Shenai, A. Soha, W.J. Spalding, L. Spiegel, S. Stoynev, J. Strait, N. Strobbe, L. Taylor, S. Tkaczyk, N.V. Tran, L. Uplegger, E.W. Vaandering, C. Vernieri, M. Verzocchi, R. Vidal, M. Wang, H.A. Weber, A. Whitbeck, Y. Wu, T. Zimmerman

University of Florida, Gainesville, U.S.A.

D. Acosta, P. Avery, P. Bortignon, D. Bourilkov, A. Brinkerhoff, A. Carnes, M. Carver, D. Curry, S. Das, R.D. Field, I.K. Furic, J. Konigsberg, A. Korytov, J.F. Low, P. Ma, K. Matchev, H. Mei, G. Mitselmakher, D. Rank, L. Shchutska, D. Sperka, L. Thomas, J. Wang, S. Wang, J. Yelton

2017 JINST 12 P04023

Florida International University, Miami, U.S.A.

S. Linn, P. Markowitz, G. Martinez, J.L. Rodriguez

Florida State University, Tallahassee, U.S.A.

A. Ackert, T. Adams, A. Askew, S. Bein, S. Hagopian, V. Hagopian, K.F. Johnson, H. Prosper, A. Santra, R. Yohay

Florida Institute of Technology, Melbourne, U.S.A.

M.M. Baarmand, V. Bhopatkar, S. Colafranceschi, M. Hohlmann, D. Noonan, T. Roy, F. Yumiceva

University of Illinois at Chicago (UIC), Chicago, U.S.A.

M.R. Adams, L. Apanasevich, D. Berry, R.R. Betts, I. Bucinskaite, R. Cavanaugh, L. Ennesser, A. Evdokimov, O. Evdokimov, L. Gauthier, C.E. Gerber, D.J. Hofman, K. Jung, S. Makauda, I.D. Sandoval Gonzalez, N. Varelas, H. Wang, Z. Wu, M. Zakaria, J. Zhang

The University of Iowa, Iowa City, U.S.A.

B. Bilki[69], W. Clarida, K. Dilsiz, S. Durgut, R.P. Gandrajula, M. Haytmyradov, V. Khristenko, J.-P. Merlo, H. Mermerkaya[70], A. Mestvirishvili, A. Moeller, J. Nachtman, H. Ogul, Y. Onel, F. Ozok[71], A. Penzo, C. Snyder, E. Tiras, J. Wetzel, K. Yi

Johns Hopkins University, Baltimore, U.S.A.

I. Anderson, B. Blumenfeld, A. Cocoros, N. Eminizer, D. Fehling, L. Feng, A.V. Gritsan, P. Maksimovic, J. Roskes, U. Sarica, M. Swartz, M. Xiao, Y. Xin, C. You

The University of Kansas, Lawrence, U.S.A.

A. Al-bataineh, P. Baringer, A. Bean, S. Boren, J. Bowen, J. Castle, L. Forthomme, R.P. Kenny III, S. Khalil, A. Kropivnitskaya, D. Majumder, W. Mcbrayer, M. Murray, S. Sanders, R. Stringer, J.D. Tapia Takaki, Q. Wang, G. Wilson

Kansas State University, Manhattan, U.S.A.

A. Ivanov, K. Kaadze, Y. Maravin, A. Mohammadi, L.K. Saini, N. Skhirtladze, S. Toda

Lawrence Livermore National Laboratory, Livermore, U.S.A.

F. Rebassoo, D. Wright

University of Maryland, College Park, U.S.A.

C. Anelli, A. Baden, O. Baron, A. Belloni, B. Calvert, S.C. Eno, C. Ferraioli, J.A. Gomez, N.J. Hadley, S. Jabeen, G.Y. Jeng, R.G. Kellogg, T. Kolberg, J. Kunkle, A.C. Mignerey, F. Ricci-Tam, Y.H. Shin, A. Skuja, M.B. Tonjes, S.C. Tonwar

Massachusetts Institute of Technology, Cambridge, U.S.A.

D. Abercrombie, B. Allen, A. Apyan, V. Azzolini, R. Barbieri, A. Baty, R. Bi, K. Bierwagen, S. Brandt, W. Busza, I.A. Cali, M. D'Alfonso, Z. Demiragli, L. Di Matteo, G. Gomez Ceballos, M. Goncharov, D. Hsu, Y. Iiyama, G.M. Innocenti, M. Klute, D. Kovalskyi, K. Krajczar, Y.S. Lai, Y.-J. Lee, A. Levin, P.D. Luckey, B. Maier, A.C. Marini, C. Mcginn, C. Mironov, S. Narayanan, X. Niu, C. Paus, C. Roland, G. Roland, J. Salfeld-Nebgen, G.S.F. Stephans, K. Tatar, M. Varma, D. Velicanu, J. Veverka, J. Wang, T.W. Wang, B. Wyslouch, M. Yang

2017 JINST 12 P04023

University of Minnesota, Minneapolis, U.S.A.

A.C. Benvenuti, R.M. Chatterjee, A. Evans, P. Hansen, S. Kalafut, S.C. Kao, Y. Kubota, Z. Lesko, J. Mans, S. Nourbakhsh, N. Ruckstuhl, R. Rusack, N. Tambe, J. Turkewitz

University of Mississippi, Oxford, U.S.A.

J.G. Acosta, S. Oliveros

University of Nebraska-Lincoln, Lincoln, U.S.A.

E. Avdeeva, K. Bloom, D.R. Claes, C. Fangmeier, R. Gonzalez Suarez, R. Kamalieddin, I. Kravchenko, A. Malta Rodrigues, J. Monroy, J.E. Siado, G.R. Snow, B. Stieger

State University of New York at Buffalo, Buffalo, U.S.A.

M. Alyari, J. Dolen, A. Godshalk, C. Harrington, I. Iashvili, J. Kaisen, D. Nguyen, A. Parker, S. Rappoccio, B. Roozbahani

Northeastern University, Boston, U.S.A.

G. Alverson, E. Barberis, A. Hortiangtham, A. Massironi, D.M. Morse, D. Nash, T. Orimoto, R. Teixeira De Lima, D. Trocino, R.-J. Wang, D. Wood

Northwestern University, Evanston, U.S.A.

S. Bhattacharya, O. Charaf, K.A. Hahn, A. Kumar, N. Mucia, N. Odell, B. Pollack, M.H. Schmitt, K. Sung, M. Trovato, M. Velasco

University of Notre Dame, Notre Dame, U.S.A.

N. Dev, M. Hildreth, K. Hurtado Anampa, C. Jessop, D.J. Karmgard, N. Kellams, K. Lannon, N. Marinelli, F. Meng, C. Mueller, Y. Musienko[38], M. Planer, A. Reinsvold, R. Ruchti, N. Rupprecht, G. Smith, S. Taroni, M. Wayne, M. Wolf, A. Woodard

The Ohio State University, Columbus, U.S.A.

J. Alimena, L. Antonelli, B. Bylsma, L.S. Durkin, S. Flowers, B. Francis, A. Hart, C. Hill, R. Hughes, W. Ji, B. Liu, W. Luo, D. Puigh, B.L. Winer, H.W. Wulsin

Princeton University, Princeton, U.S.A.

S. Cooperstein, O. Driga, P. Elmer, J. Hardenbrook, P. Hebda, D. Lange, J. Luo, D. Marlow, T. Medvedeva, K. Mei, I. Ojalvo, J. Olsen, C. Palmer, P. Piroué, D. Stickland, A. Svyatkovskiy, C. Tully

University of Puerto Rico, Mayaguez, U.S.A.

S. Malik

Purdue University, West Lafayette, U.S.A.

A. Barker, V.E. Barnes, S. Folgueras, L. Gutay, N. Hinton, M.K. Jha, M. Jones, A.W. Jung, A. Khatiwada, D.H. Miller, N. Neumeister, J.F. Schulte, X. Shi, J. Sun, F. Wang, W. Xie

Purdue University Calumet, Hammond, U.S.A.

N. Parashar, J. Stupak

Rice University, Houston, U.S.A.

A. Adair, B. Akgun, Z. Chen, K.M. Ecklund, F.J.M. Geurts, M. Guilbaud, M. Kilpatrick, W. Li, B. Michlin, M. Northup, T. Nussbaum, B.P. Padley, J. Roberts, J. Rorie, Z. Tu, J. Zabel

2017 JINST 12 P04023

University of Rochester, Rochester, U.S.A.

B. Betchart, A. Bodek, P. de Barbaro, R. Demina, Y.t. Duh, T. Ferbel, M. Galanti, A. Garcia-Bellido, J. Han, O. Hindrichs, A. Khukhunaishvili, K.H. Lo, P. Tan, M. Verzetti

Rutgers, The State University of New Jersey, Piscataway, U.S.A.

A. Agapitos, J.P. Chou, Y. Gershtein, T.A. Gómez Espinosa, E. Halkiadakis, M. Heindl, E. Hughes, S. Kaplan, R. Kunnawalkam Elayavalli, S. Kyriacou, A. Lath, K. Nash, M. Osherson, M. Park, H. Saka, S. Salur, S. Schnetzer, D. Sheffield, S. Somalwar, R. Stone, S. Thomas, P. Thomassen, M. Walker

University of Tennessee, Knoxville, U.S.A.

A.G. Delannoy, M. Foerster, J. Heideman, G. Riley, K. Rose, S. Spanier, K. Thapa

Texas A&M University, College Station, U.S.A.

O. Bouhali[72], A. Celik, M. Dalchenko, M. De Mattia, A. Delgado, S. Dildick, R. Eusebi, J. Gilmore, T. Huang, E. Juska, T. Kamon[73], R. Mueller, Y. Pakhotin, R. Patel, A. Perloff, L. Perniè, D. Rathjens, A. Safonov, A. Tatarinov, K.A. Ulmer

Texas Tech University, Lubbock, U.S.A.

N. Akchurin, C. Cowden, J. Damgov, F. De Guio, C. Dragoiu, P.R. Dudero, J. Faulkner, E. Gurpinar, S. Kunori, K. Lamichhane, S.W. Lee, T. Libeiro, T. Peltola, S. Undleeb, I. Volobouev, Z. Wang

Vanderbilt University, Nashville, U.S.A.

S. Greene, A. Gurrola, R. Janjam, W. Johns, C. Maguire, A. Melo, H. Ni, P. Sheldon, S. Tuo, J. Velkovska, Q. Xu

University of Virginia, Charlottesville, U.S.A.

M.W. Arenton, P. Barria, B. Cox, J. Goodell, R. Hirosky, A. Ledovskoy, H. Li, C. Neu, T. Sinthuprasith, X. Sun, Y. Wang, E. Wolfe, F. Xia

Wayne State University, Detroit, U.S.A.

C. Clarke, R. Harr, P.E. Karchin, J. Sturdy

University of Wisconsin - Madison, Madison, WI, U.S.A.

D.A. Belknap, J. Buchanan, C. Caillol, S. Dasu, L. Dodd, S. Duric, B. Gomber, M. Grothe, M. Herndon, A. Hervé, P. Klabbers, A. Lanaro, A. Levine, K. Long, R. Loveless, T. Perry, G.A. Pierro, G. Polese, T. Ruggles, A. Savin, N. Smith, W.H. Smith, D. Taylor, N. Woods

†: Deceased
1: Also at Vienna University of Technology, Vienna, Austria
2: Also at State Key Laboratory of Nuclear Physics and Technology, Peking University, Beijing, China
3: Also at Institut Pluridisciplinaire Hubert Curien (IPHC), Université de Strasbourg, CNRS/IN2P3, Strasbourg, France
4: Also at Universidade Estadual de Campinas, Campinas, Brazil
5: Also at Universidade Federal de Pelotas, Pelotas, Brazil
6: Also at Université Libre de Bruxelles, Bruxelles, Belgium
7: Also at Deutsches Elektronen-Synchrotron, Hamburg, Germany
8: Also at Joint Institute for Nuclear Research, Dubna, Russia

2017 JINST 12 P04023

9: Now at Cairo University, Cairo, Egypt
10: Also at Fayoum University, El-Fayoum, Egypt
11: Now at British University in Egypt, Cairo, Egypt
12: Now at Ain Shams University, Cairo, Egypt
13: Also at Université de Haute Alsace, Mulhouse, France
14: Also at Skobeltsyn Institute of Nuclear Physics, Lomonosov Moscow State University, Moscow, Russia
15: Also at Tbilisi State University, Tbilisi, Georgia
16: Also at CERN, European Organization for Nuclear Research, Geneva, Switzerland
17: Also at RWTH Aachen University, III. Physikalisches Institut A, Aachen, Germany
18: Also at University of Hamburg, Hamburg, Germany
19: Also at Brandenburg University of Technology, Cottbus, Germany
20: Also at Institute of Nuclear Research ATOMKI, Debrecen, Hungary
21: Also at MTA-ELTE Lendület CMS Particle and Nuclear Physics Group, Eötvös Loránd University, Budapest, Hungary
22: Also at Institute of Physics, University of Debrecen, Debrecen, Hungary
23: Also at Indian Institute of Technology Bhubaneswar, Bhubaneswar, India
24: Also at University of Visva-Bharati, Santiniketan, India
25: Also at Indian Institute of Science Education and Research, Bhopal, India
26: Also at Institute of Physics, Bhubaneswar, India
27: Also at University of Ruhuna, Matara, Sri Lanka
28: Also at Isfahan University of Technology, Isfahan, Iran
29: Also at Yazd University, Yazd, Iran
30: Also at Plasma Physics Research Center, Science and Research Branch, Islamic Azad University, Tehran, Iran
31: Also at Università degli Studi di Siena, Siena, Italy
32: Also at Laboratori Nazionali di Legnaro dell'INFN, Legnaro, Italy
33: Also at Purdue University, West Lafayette, U.S.A.
34: Also at International Islamic University of Malaysia, Kuala Lumpur, Malaysia
35: Also at Malaysian Nuclear Agency, MOSTI, Kajang, Malaysia
36: Also at Consejo Nacional de Ciencia y Tecnología, Mexico city, Mexico
37: Also at Warsaw University of Technology, Institute of Electronic Systems, Warsaw, Poland
38: Also at Institute for Nuclear Research, Moscow, Russia
39: Now at National Research Nuclear University 'Moscow Engineering Physics Institute' (MEPhI), Moscow, Russia
40: Also at St. Petersburg State Polytechnical University, St. Petersburg, Russia
41: Also at University of Florida, Gainesville, U.S.A.
42: Also at California Institute of Technology, Pasadena, U.S.A.
43: Also at INFN Sezione di Padova; Università di Padova; Università di Trento (Trento), Padova, Italy
44: Also at Budker Institute of Nuclear Physics, Novosibirsk, Russia
45: Also at Faculty of Physics, University of Belgrade, Belgrade, Serbia
46: Also at INFN Sezione di Roma; Università di Roma, Roma, Italy
47: Also at University of Belgrade, Faculty of Physics and Vinca Institute of Nuclear Sciences, Belgrade, Serbia
48: Also at Scuola Normale e Sezione dell'INFN, Pisa, Italy
49: Also at National and Kapodistrian University of Athens, Athens, Greece
50: Also at Riga Technical University, Riga, Latvia
51: Also at Institute for Theoretical and Experimental Physics, Moscow, Russia
52: Also at Albert Einstein Center for Fundamental Physics, Bern, Switzerland

2017 JINST 12 P04023

53: Also at Adiyaman University, Adiyaman, Turkey
54: Also at Istanbul Aydin University, Istanbul, Turkey
55: Also at Mersin University, Mersin, Turkey
56: Also at Cag University, Mersin, Turkey
57: Also at Piri Reis University, Istanbul, Turkey
58: Also at Ozyegin University, Istanbul, Turkey
59: Also at Izmir Institute of Technology, Izmir, Turkey
60: Also at Marmara University, Istanbul, Turkey
61: Also at Kafkas University, Kars, Turkey
62: Also at Istanbul Bilgi University, Istanbul, Turkey
63: Also at Yildiz Technical University, Istanbul, Turkey
64: Also at Hacettepe University, Ankara, Turkey
65: Also at Rutherford Appleton Laboratory, Didcot, United Kingdom
66: Also at School of Physics and Astronomy, University of Southampton, Southampton, United Kingdom
67: Also at Instituto de Astrofísica de Canarias, La Laguna, Spain
68: Also at Utah Valley University, Orem, U.S.A.
69: Also at Argonne National Laboratory, Argonne, U.S.A.
70: Also at Erzincan University, Erzincan, Turkey
71: Also at Mimar Sinan University, Istanbul, Istanbul, Turkey
72: Also at Texas A&M University at Qatar, Doha, Qatar
73: Also at Kyungpook National University, Daegu, Korea

2017 JINST 12 P04023